

Worcester Polytechnic Institute Digital WPI

Major Qualifying Projects (All Years)

Major Qualifying Projects

May 2014

Transparent Tissue Preparation

Bielinsky Alberto Brea
Worcester Polytechnic Institute

Danny Mauricio Flores Castro
Worcester Polytechnic Institute

Follow this and additional works at: <https://digitalcommons.wpi.edu/mqp-all>

Repository Citation

Brea, B. A., & Flores Castro, D. M. (2014). *Transparent Tissue Preparation*. Retrieved from <https://digitalcommons.wpi.edu/mqp-all/23>

This Unrestricted is brought to you for free and open access by the Major Qualifying Projects at Digital WPI. It has been accepted for inclusion in Major Qualifying Projects (All Years) by an authorized administrator of Digital WPI. For more information, please contact digitalwpi@wpi.edu.

Transparent Tissue Preparation

Bielinsky Brea
Danny Flores

Ming Su, Ph.D.
Department of Biomedical Engineering

**Major Qualifying Project
2013-2014
Department of Biomedical Engineering
Worcester Polytechnic Institute**

Table of Contents

Authorship	6
Acknowledgements.....	7
Abstract.....	8
Chapter 1 Introduction	9
1.1 Background	10
Chapter 2 Literature Review	14
2.1 Cancer Background.....	15
2.1.1 Carcinogenesis	15
2.1.2 Symptoms.....	18
2.1.3 Costs	19
2.1.4 Treatment.....	21
2.2 Tumor Heterogeneity	24
2.2.1 Causes and Effects.....	25
2.2.2 Effects on Cancer Treatment.....	26
2.3 Project Significance.....	26
2.3.1 Current Issues.....	27
2.3.2 Personalized Approach.....	28
2.4 Technical Background	28
2.4.1 Transparency	29
2.4.2 Proteins in Tumors.....	31
2.4.3 Imaging Proteins	32
2.5 Related Methods	33
2.5.1 The Cancer Genome Atlas	33
2.5.2 Zebrafish Study	35
2.5.3 Tissue on Collagen I-Hydrogel Scaffold	36
2.5.4 Scale	39
2.5.5 CLARITY	42
2.5.6 SeeDB	46
2.5.7 Supercritical CO ₂	48
Chapter 3 Project Strategy	50
3.1 Initial Client Statement.....	51

3.2 Objectives.....	52
3.3 Constraints	54
3.4 Revised Client Statement.....	54
3.5 Project Approach	55
3.5.1 Technical Approach.....	55
3.5.2 Design Evaluation Matrix.....	55
3.5.3 Design Functions and Specifications.....	56
Chapter 4 Alternative Designs	58
4.1 Needs Analysis.....	59
4.2 Conceptual Designs.....	61
4.2.1 Clearing Agent as a Solvent.....	61
4.2.2 Optical Clearing through Electrical leaching	62
4.2.3 Supercritical CO2 for lipid extraction.....	62
4.3 Design Modeling.....	63
4.4 Feasibility Study.....	66
4.4.1 Preliminary Data	68
4.5 Final Design.....	70
Chapter 5 Methodology (Design Validation).....	72
5.1 SFE Chamber	73
5.2 Hydrogel Scaffold.....	74
5.3 Supercritical Fluid Extraction Setup.....	74
5.3.1 Pressure test.....	75
5.3.2 Temperature test.....	75
5.3.3 Leaks test.....	75
5.4 Experimental setup.....	76
5.5 Transparency Assessment.....	77
Chapter 6 Results	78
6.1 Absorbance Test Results	79
6.2 Results on SFE Chamber extraction.....	80
Chapter 7 Discussion	81
Chapter 8 Conclusions and Future Recommendations	85
8.1 Add Heating system.....	86
8.2 Incorporate self-refilling dry ice	87

8.3 Improve Closing mechanism.....	87
8.4 Expand SFE chamber	88
8.5 Implementing Fluorescent Staining.....	88
References	89
Appendix	95

Table of Figures

Figure 1: Pyrimidine dimers [16].....	17
Figure 2: Double strand breakage [17].....	17
Figure 3: Worldwide causes of death in 2004[21].....	20
Figure 4: Objectives of chemotherapy[27].....	22
Figure 5: Example of the configuration of common radiation therapy in a clinic [30].....	23
Figure 6: Results for the study done at UAB. This is the distribution of the 89 medication errors [41].	27
Figure 7: Lipid bilayer in human cells [44].....	30
Figure 8: Transmission fraction and Intensity values of light traveling through mouse brain cells with lipid bilayer membrane [45].	30
Figure 9: Results obtained in the NIH experiment. Notice how at later stages of cancer, more CPE- Δ N is found to be present in tumors [47].	32
Figure 10:Circos Plot. Outer ring represents the chromosomes and Inner rings represent the locations of different types of mutations [6].....	34
Figure 11:Transparent Adult Zebrafish [51].....	35
Figure 12: Advantages of Zebrafish based on it's lifecycle [51].	36
Figure 13: Collagen I hydrogel cultured with MDA-MB 231 [52].....	37
Figure 14:MDA-MB-231 cells cultured in collagen I hydrogel for a week [52].....	38
Figure 15: Tumor Necrosis due to Hypoxia [52].	38
Figure 16: Two mouse embryos after fixation, left fixated in PBS and right in ScaleA2 for two weeks	39
Figure 17: Light Transmittance of ScaleA2, 60% Sucrose/PBS, Focus/MountClear, and PBS [53].	40
Figure 18:Mouse brain before and after ScaleA2 (two weeks) [53].....	41
Figure 19:ScaleA2 steps for tissue transparency for deep imaging [53].....	42
Figure 20: Infusion of monomer (blue), formaldehyde (red) and tissue.	43
Figure 21: Creation of hydrogel mesh by incubation [8].	43
Figure 22:Removal of lipids by using SDS detergent and a voltage [8].....	44
Figure 23: ETC Chamber Diagram [8].	44
Figure 24: Actual ETC Chamber made from Nalgene Bottle.....	45
Figure 25: Images of 4 Month Old Mouse Brains. (A) Before ETC Chamber (B) Scale method for 5 weeks (C) CLARITY method for 2 days (D) Fluorescent image of C	45

Figure 26:3D Map of Stained Hippocampus. Blue areas are supporting glia, red areas are connecting interneurons, and green areas are fluorescent-expressing neurons [8].....	46
Figure 27: Refractive index equation. c = speed of light in a vacuum v =speed of light in the substance [54].....	47
Figure 28: Various tissues before and after SeeDB [55].....	47
Figure 29: Phase Diagram of Carbon Dioxide (based on Pressure and Temperature) [57].....	48
Figure 30: Comparison of supercritical extraction and solvent extraction [58].	49
Figure 31: Supercritical Fluid Extraction Diagram [58].	49
Figure 32: Objectives Tree	52
Figure 33: CAD model of the supercritical fluid extraction chamber.....	64
Figure 34: CAD model of the lower extraction chamber.	64
Figure 35: Assembly of the SFE chamber.	67
Figure 36: UV-Vis absorbance spectra of the extract obtained from the orange samples. The original absorbance plot is on the left, while the smoothed absorbance plot is on the right. ...	69
Figure 37: UV-Vis spectra of the reference limonene.....	70
Figure 38: Absorbance plots for the orange oil extract obtained in our experiments (left) and the reference limonene (right). For the plot of the reference limonene, the reference limonene absorbance graph is represented by the solid black line.....	79
Figure 39: Porcine liver samples before and after extraction.....	80

Table of Tables

Table 1: Pairwise Comparison Chart	52
Table 2: Design Evaluation Matrix.....	56
Table 3: Defined Needs and Wants table	60
Table 4: Specification table for the materials used to build the SFE chamber.	65

Authorship

Both team members contributed equally to all sections included in the report.

Acknowledgements

Our team would like to thank the following individuals for contributing in our Project:

- Professor Ming Su in the Biomedical Engineering Department for advising the project and providing important resources for the project's completion.
- Chaoming Wang of the Su Lab for his immense support and guidance throughout the project.
- Professor Ambady Sakthikumar in the Biomedical Engineering Department for his support with logistics.
- Lisa Wall for being a great source for resources and logistics.
- Jonathan Labrie for assisting countless times in the machining process.
- Laura Hanlan for helping our team in the research parts of the project.

Abstract

A common issue in cancer treatment is the lack of understanding of the heterogeneous chemical composition within individual tumors. It is known that several lipid bilayer extraction techniques allow molecular signals to be detected through microscopy as the tissue becomes less opaque. The goal of this project was to develop a method that could effectively remove lipid bilayer membranes from tissues. To accomplish this, a Supercritical Fluid Extraction (SFE) technique with supercritical CO₂ was used to remove lipids from porcine tissue. The results compare the transparency level of tissue undergoing SFE before and after treatment. Given the data obtained in the experiments, it can be concluded that SFE using CO₂ has potential as a mechanism of lipid extraction for future verification of tumor heterogeneity.

Chapter 1

Introduction

1.1 Background

Cancer is known worldwide as one of the most deadly diseases, if not the deadliest, to affect humans. The toll that cancer has on human life is ever-increasing. In 2008, approximately 7.6 million people died because of cancer. It is expected that by 2015, 9 million people will perish from this condition [1]. Furthermore, cancer also brings an economical toll to those families whose members suffer from this condition. Many of the medicines currently used to treat cancer can rise above the \$50,000 mark, over the course of the treatment. In fact, some drugs, such as Erbitux (a drug used to treat colorectal, head, and neck cancer), cost as high as \$9600 per month [2]. Considering that oftentimes insurance companies do not offer their help to cover for complete costs, there is currently much work done to develop better techniques to treat cancer.

In order to understand why cancer is such a costly disease, it is important to understand the pathways that lead to cancer and the effects that cancer has on the body. Cancer occurs when a cell's DNA suffers significant damage and the cell does not repair the damage in its DNA. Under normal conditions, this damaged DNA, or mutation, would lead to DNA repair and/or cell apoptosis. Under cancer conditions however, the cell's genome forces the normal cell to transform into a cancer cell, bringing forth a series of changes within the cell: increased and varied protein synthesis, abnormal growth, loss of function in the tissue and, in some cases, migration from the tissue. The causes of cancer may be categorized as either hereditary or carcinogenic [3]. When cancer is hereditary, a mutated gene in a person's DNA is passed to future generations, effectively increasing the risk of cancer development in that person's children. Carcinogens, such as certain types of radiation or chemical substances, can also affect DNA inside the cell. Once cancer cells have been transformed inside the body, a tumor is formed. Releasing hormones that alter tissue function and obstruct flow of substances causes damage to the tissue. When tumor cells detach themselves from the tumor,

metastasis occurs. In metastatic cancer, tumor cells have grown and developed sufficiently to travel to other parts of the body. A common example of cancer metastasis occurs in breast cancer. Breast cancer cells often travel to the lymph nodes located in the underarm, thus making treatment much more difficult because of the multiple locations of cancer cells in the body [4]. Additionally, cancer cells within a tumor do not have identical genetic identities, making cancer treatment the more difficult. Since cancer cells reproduce faster than normal cells, their genome very oftentimes undergoes rapid changes from generation to generation. This means that as a cancer cell reproduces, genetic variety in the offspring cells causes each cell to be different from each other. In more technical terms, each cancer cell derived from a single parent cell can produce its own set of its proteins and enzymes allowing each cell to have a different phenotype from other cells from their same generation. This difference in cancer cells within a single tumor is what is called tumor heterogeneity. Tumor heterogeneity is what makes cancer types differ so much from patient to patient. It is the reason why cancer treatments need to be often tailored to a single patient, since the biochemical properties inside that patient's tumor are unique to his/her tumor.

Knowing the variety in cancer types has allowed doctors and patients alike to treat cancer with a variety of methods. The most known methods involve the use of drugs to target cancer cells and either stop them from growing or kill them. This kind of drug treatment, known as chemotherapy, is widely used around the world as it offers close control of the drug being taken. However, control in chemotherapy does not always result in the desired outcome since the patient's response to the drug cannot be controlled. Many drugs have unknown adverse side-effects that vary from patient to patient [5]. These effects often result in painful side effects that effectively kill cancer cells while at the same time affecting normal cells in the patient's body. Furthermore, the high cost of some of these drugs might imply that chemotherapy might not always prove to be the best way to treat cancer by itself. Other

effective cancer treatment methods such as radiation therapy and immunotherapy also focus on targeting the cancer cells specifically. At this point in time however, no method has proven to be 100% effective and infallible. There is a need to design novel methods to treat cancer that will allow a patient to receive harmless and effective treatment at the same time.

The goal of this project is to create a method that will allow for a reliable and quick check of the protein composition of tumors in patients suffering from cancer. Given the current state of cancer treatment, along with the high cost associated with cancer, our team has identified an issue in the way treatment is performed in the modern days. Although methods such as chemotherapy and radiation therapy involve consideration of various factors inherent to the patient (such as weight, metabolism, blood count, past diseases), the majority of these methods often do not take into account the difference within the patient's tumor. That is, tumor heterogeneity is not always a factor that many of the current cancer treatment methods take into account. Even though there exist programs, such as The Cancer Genome Atlas (TCGA), which attempt to categorize cancers in terms of genetic composition, there is no method that can actually identify tumor composition in a fast and effective manner [6]. However, there have been methods created in the recent years that provide an idea to perform protein labeling and protein visualization within a tumor. Methods such as immunoblotting and 3D fluorescence techniques allow for protein recognition and labeling [7]. Methods involving the use of chemical reagents and electrical leaching to remove lipids from cells allow for tissue to become almost transparent allowing for much easier 3D visualization [8 and 9]. These types of methods will provide the technical context for the development of the method in this project.

To create such method, the project strategy to be employed will focus on developing a multi-step process that will allow clinicians to determine heterogeneity in tumors in a quick and effective manner. The strategy for this project is to begin looking at past experiments

related to tumor heterogeneity, cancer treatment, and protein labeling within transparent tissue. Once research on related techniques has been done, a process will be developed so that tumor tissue can be properly embedded into a scaffold. In the final design, it is intended to obtain tumor tissue from a tumor biopsy of a cancer patient. Once the tissue is in the scaffold, the lipid bilayer of the tumor cells will be removed. Without the lipid bilayer membrane, the tumor cells will allow visible light to go through them. This will then allow the visualization of proteins once these proteins have been fluorescently labeled. Proteins will then be identified by clinicians, and treatment strategies will be formulated based on the specific proteins found within the tumor.

Chapter 2

Literature Review

2.1 Cancer Background

Cancer is one of the most deadly conditions that affect the human body. In the US, cancer is the second most fatal disease behind heart failure. The toll of cancer is also heavy around the globe. In 2004, 7.4 million deaths were registered as being caused by cancer, this being a 12.6% of the total deaths estimated in that year [10]. Cancer is also one of the most troublesome diseases to treat because it is not caused by a particular condition and it is not location-specific. Cancer begins as the DNA inside a cell becomes damaged by one of the many pathways that lead to cancer. These pathways are referred to as carcinogens, and they can be either substances or radiation that damages the genetic composition of the cell. Cancer can also be a hereditary condition. Parents who have often suffered from cancer might end up having offspring who may develop the condition at any time during their lifetime. And since cancer is a disease that does not originate in the same part of the body for all patients, cancer has become a complex disease to treat once it has progressed inside the body.

2.1.1 Carcinogenesis

Cancer begins as a single cell in tissue becomes altered by an environmental or hereditary factor [11]. Environmental factors refer to any of those factors that are not genetically inherited. Factors such as chemicals, infections, and radiation can all be considered environmental since they can all cause DNA mutations. These factors, referred to as carcinogens, most often affect the cell's DNA by damaging a particular gene that encodes against tumor initiation. For example, a particular gene known as TP53 is oftentimes inactivated by a protein created by the genetic code in the human papilloma virus (HPV). TP53 is a tumor suppressor gene that can regulate DNA repair proteins and initiate apoptosis in the cell in case DNA damage is severe [12]. Other carcinogens might affect gene function by forcing a gene to overexpress a particular protein that promotes cell growth or proliferation.

Such genes, known as proto-oncogenes, might become oncogenes, or genes that code for a protein that will initiate cancer. Contrary to environmental factors, hereditary factors are those that arise from hereditary conditions meaning that they are passed from parents to their offspring. Gene defects passed down from parents are very often the cause of hereditary cancers. In breast cancers for example, it is known that the inherited mutation in BRCA genes can lead to the development of cancer accounted for more than 75% of breast cancer cases [13].

Carcinogenesis, the term used to refer to the growth of cancer cells, occurs when either environmental or hereditary factors cause damage to the DNA of a single cell. Most of the time, a cell is capable of repairing the damage in its DNA. In other cases, if the damage is irreversible, the cell's DNA triggers the production of proteins necessary for the cell to undergo apoptosis. Carcinogenesis happens when either of these pathways (DNA repair or cell apoptosis) fails to be executed properly. In many cases, the environmental carcinogens lead to a mutation in a specific gene in the DNA that can code for a repair protein. For example, ultraviolet radiation known as UVB can affect DNA by causing malfunctions of entire genes. UVB can cause single-strand damages in pyrimidine monomers (Figure 1), or double stranded breakage (Figure 2) which often accounts for deleted genes [14 and 15].

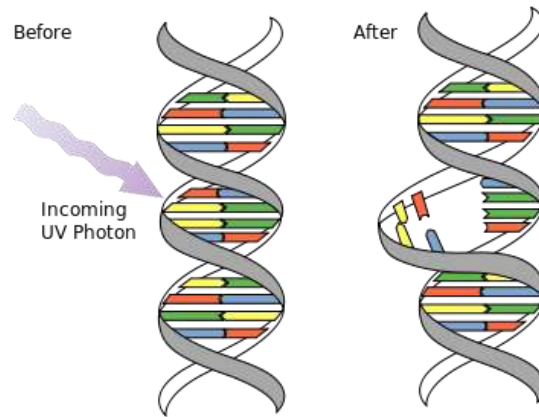


Figure 1: Pyrimidine dimers [16].

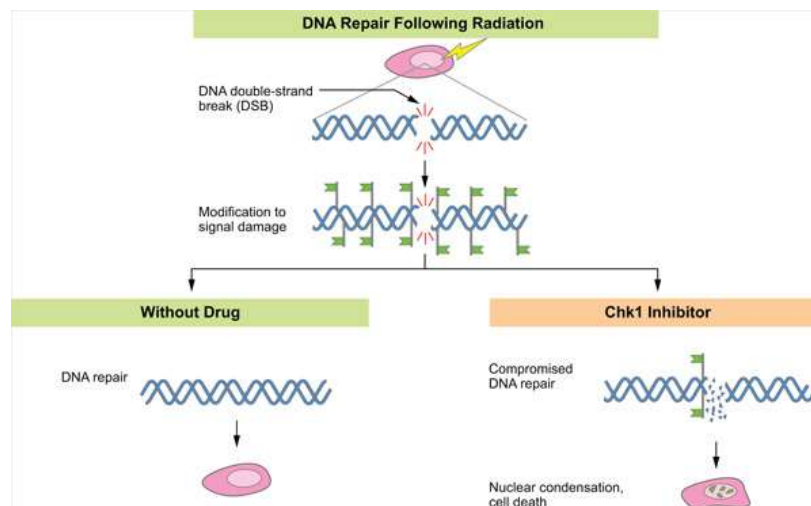


Figure 2: Double strand breakage [17].

Hereditary factors lead to carcinogenesis as altered genes in parents are passed down to their children. In many cancers, inactivated tumor suppressor genes like the one coding for the APC protein (adenomatous polyposis coli), appear in the offspring genome. The APC gene codes for the APC protein which regulates cell growth, proliferation and movement of colorectal cells. In the cases of people who have inherited the inactivated APC gene, by the time they reach the age of 40, the probability of getting colorectal cancer is almost 100% [18]. While inherited mutations in genes do not always lead straightly to carcinogenesis, other

pathologies might cause further mutations in the individual which can eventually trigger the carcinogenic pathway.

2.1.2 Symptoms

Once a cell has become a cancer cell, or transformed, the effects of this transformation are spread to the surrounding tissue. At the early stages of cancer, when the cell has just begun growth and early duplication, no apparent symptoms may be perceived by the patient. However, as the original cancer cell undergoes several rounds of duplication and the number of cancer cells increases, a tumor, or neoplasm, is formed. Neoplasms, which refer to the abnormal growth and accumulation of tissue, are often responsible for the earliest symptoms related to cancer. Many tumors, such as the ones that grow in the pancreas, cause no symptom until these tumors grow in size and begin to push against the nerve endings in the tissue. In other more sensitive organs however, tumors of the smallest of sizes might cause symptoms as soon as the organ's functions become interrupted by the presence of the tumor. This is the case of tumors that grow in the brain or lung, where a slight disturbance in those organs might cause headaches or heavy coughing. In fact, most of the common symptoms associated to other common diseases include headaches, tiredness, fever, and weight loss. The more specific symptoms of tumor presence are always dependent on the location of the tumor. Examples of specific symptoms of cancer are: lump(s) in the body, strong cough or hoarseness, difficulty in swallowing, abnormal bleeding, difficulty in urinating, and changes in bowel movement. [19 and 20]

As the cancer progresses, oftentimes cancer cells undergo a process known as metastasis. This refers to the cells acquiring the ability to de-attach from the tissue matrix that binds them to their tissue. Metastatic cancer cells are what make cancer so deadly. These cells usually de-attach from the tumor and travel through the vessels of the circulatory and

lymphatic system. As these metastatic cells move through the body, they end up settling in a body part different from the one they originated. As the metastatic cell settles and replicates in the new tissue, a new tumor will form in tissue different from the original. In cases where metastasis occurs, symptoms of metastasis only become apparent once a new tumor begins to form. In the majority of cases, metastasis is a signal of a very advanced stage of cancer. At a metastatic cancer stage, priority is given in pointing out the locations where cancer cells might have settled so that treatment can be given to the patient. Symptoms associated with tumor metastasis are often a replica of when cancer was first diagnosed, though with the added intensity of being a second (or even third) time.

2.1.3 Costs

The American Cancer Association (ACA) shows in their Global Facts and Figures that in 2004, about 7.4 million people died of cancer worldwide. It also shows that 5.2 million people out of those 7.4 million died in developing countries whereas the remaining 2.2 million died in developed countries. Out of the many diseases that claimed human lives in that year, such as HIV/AIDS, malaria, diabetes, and pulmonary diseases, cancer was the second deadliest disease behind heart failure. [21]

Table 1. Leading Causes of Death Worldwide and in Developing and Developed Countries, 2004 (thousands)

	Worldwide			Developing			Developed		
	Rank	Deaths	%	Rank	Deaths	%	Rank	Deaths	%
Heart diseases	1	8,923	15.1	1	7,342	14.5	2	1,563	19.3
Malignant neoplasms	2	7,424	12.6	2	5,255	10.4	1	2,154	26.6
Cerebrovascular diseases	3	5,712	9.7	3	4,949	9.8	3	757	9.4
Lower respiratory infections	4	4,177	7.1	4	3,910	7.7	4	305	3.8
Perinatal conditions*	5	3,180	5.4	5	3,141	6.2		35	0.4
Chronic obstructive pulmonary disease	6	3,025	5.1	6	2,737	5.4	5	285	3.5
Diarrhoeal diseases	7	2,163	3.7	7	2,148	4.2		14	0.2
HIV/AIDS	8	2,040	3.5	8	2,018	4.0		20	0.2
Tuberculosis	9	1,464	2.5	9	1,448	2.9		15	0.2
Road traffic accidents	10	1,275	2.2	10	1,158	2.3		114	1.4
Diabetes mellitus	11	1,141	1.9		914	1.8	7	221	2.7
Malaria	12	889	1.5		888	1.8		0	0.0
Suicide	13	844	1.4		707	1.4	9	118	1.5
Cirrhosis of the liver	14	772	1.3		655	1.3	10	116	1.4
Nephritis and nephrosis	15	739	1.3		611	1.2	8	126	1.6
All causes		58,772	100.0		50,582	100.0		8,095	100.0

The number zero in a cell indicates a non-zero estimate of less than 500.

* Includes "causes arising in the perinatal period" as defined in the International Classification of Diseases, principally low birthweight, prematurity, birth asphyxia, and birth trauma, and does not include all causes of deaths occurring in the perinatal period.

Source: World Health Organization, The global burden of disease: 2004 update.

Figure 3: Worldwide causes of death in 2004[21].

In the United States alone, 1,638,910 new cancer cases were reported in a 2012 ACA document. Out of all those cases, 577,190 people died of cancer in 2012, a 35% of the total 1,638,910. An estimated distribution of 52% male deaths against 48% female deaths also shows that cancer affects men and women similarly. [21]

Aside from the human loss, financial loss is also great in the cancer treatment area. The ACA reports that in 2007, about \$ 103.8 billion were invested in cancer care alone in the United States [21]. The National Cancer Institute reports that in 2010 about \$124.5 billion were invested in cancer care, and that by 2020 it is expected that \$158 billion (in 2010 dollars) will be spent in cancer care [21]. In terms of single drugs or treatment, cancer is also one of the most expensive conditions to treat. Drugs such as Avastin can cost as high as \$55,000 per year, whereas therapies such as proton therapy radiation can cost as high as \$50,000 per session [22 and 23].

2.1.4 Treatment

As mentioned before, costs associated with cancer treatment are often very high. This is often the case because of the equipment and technology used to treat cancer patients. In many cases, a single individual must undergo a series of combined therapies that will try to minimize the effects of cancer on the patient. Most of the time these therapies target the cancer cells directly since these therapies attempt to kill these cells. Other therapies however, help the patient by identifying the size of the tumor in the patient and by minimizing the symptoms caused by cancer. [24]

2.1.4.1 Chemotherapy

Chemotherapy refers to the use of drugs to destroy cancer cells or to reduce the symptoms caused by cancer and other cancer therapies. Chemotherapy has been used since the early 1950's to treat cancer and has proved to be an effective therapy ever since [25]. Normally, the drugs used for chemotherapy attempt to damage the DNA in the cells in order to prevent growth and proliferation. The types of drugs used for chemotherapy include: alkylating agents, antimetabolites, anti-tumor antibiotics, enzyme inhibitors, and corticosteroids among others. Some of these drugs have major adverse side effects such as heart complications, secondary cancer, and peripheral nervous system damage. Since most of these drugs do not specifically target tumor cells, the normal cells that surround the tumor tissue might also be affected by the drug. [26].

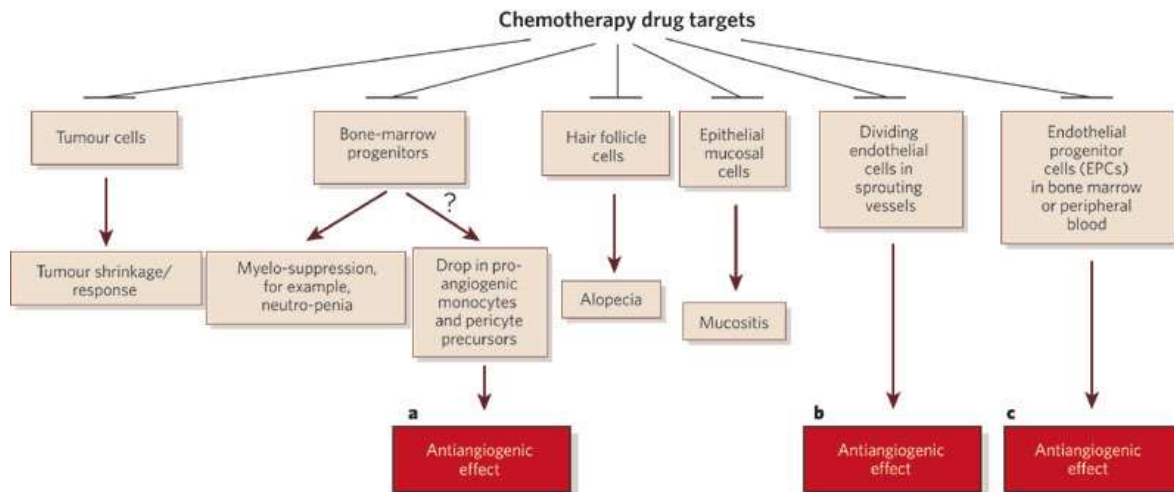


Figure 4: Objectives of chemotherapy [27].

2.1.4.2 Radiation therapy

Radiation therapy refers to the kind of treatment that involves the use of radiation to destroy cancer cells. The type of radiation used to treat cancer involves high doses of ionizing radiation such as x-ray or gamma rays. These rays are capable of damaging the DNA structure of cells so that they do not grow or reproduce. The types of radiation used against cancer are photon radiation and particle radiation. Photon radiation refers to the types of radiation which come from radioactive sources such as cobalt, cesium, or from a machine called linear accelerator. In photon radiation, the ions produced in the DNA atoms damage the structure of the double-stranded DNA. Particle radiation refers to the use of subatomic particles which cause damage to the cancer cells' DNA. Electron beams, proton beams, neutron beams, and ion radiation are all examples of types of particle radiation. These types of radiation can be used for a variety of cancer types. Electron beams are mostly used to treat skin cancers since they do not penetrate deep in the body. Neutron beams and carbon ion radiation are stronger types of radiation that are used to attack cancer cells deep within tissue. Nonetheless,

radiation still poses a threat to the normal tissue surrounding the cancer cells, since radiation damages all cell's DNA equally. [28 and 29]



Figure 5: Example of the configuration of common radiation therapy in a clinic [30].

2.1.4.3 Surgery

Surgery is mainly done in cancer in order to extract biopsies or tumors from the patient's body. Surgery has some other applications which can help prevent cancer or diagnose the extent at which cancer has grown in the body. Some of the types of surgery are preventive surgery, diagnostic surgery, curative surgery, and debulking surgery. Preventive surgery as the name suggests, is used to prevent the formation of tumors by removing tissue which is very prone to becoming cancerous. Diagnostic surgery is used to extract a part of tumor tissue in order to identify the kind of cancer inside the patient's body. Curative surgery and debulking surgery can be used to remove tumor from the patient to either attempt to cure or to reduce the size and effects of the tumor inside the body. [31]

2.1.4.4 Other methods

Aside from the three most common methods used to treat cancer, there are other methods that can provide assistance in cancer treatment. Some of these methods are immunotherapy, photodynamic therapy, and targeted therapy. Immunotherapy is the use of the body's own immune system to target and attack cancer cells. This is done by using antibodies or vaccines which can then help the body's immune system target and destroy cancer cells once they start growing [32]. Photodynamic therapy uses specialized drugs, called photosensitizing agents, and light to kill cancer cells. These photosensitizing agents, once inside the cancer cells, kill cancer cells as they react with oxygen inside the cells after light has been applied on the tumor site. Targeted therapy is similar to chemotherapy in that it uses drugs to target cancer cells. Targeted therapy however, allows for these drugs to attack cancer cells while causing minor damage to the surrounding normal cells. [24]

2.2 Tumor Heterogeneity

Tumor heterogeneity refers to the biochemical variability that exists in single tumors in a cancer patient. Tumor differences exist in individual tumors because of the phenotype differences that cancer cells express within the tumor. Some of these differences include antigen expression, membrane composition, response to chemotherapy, and metastatic proclivity [33]. However, there are other views that refer to tumor heterogeneity as the difference in cell lineage that give rise to different types of cancer cells. Regardless of the point of view, tumor heterogeneity provides an important explanation of why current cancer treatment methods do not always provide a cure for cancer.

2.2.1 Causes and Effects

There are many causes of tumor heterogeneity. One of the causes of tumor heterogeneity is believed to be related to the developmental changes that cancer cells undergo as they grow in tissue. Studies have shown that normal cells, prior to becoming cancer cells, are also heterogeneous among themselves [34]. The different carcinogen susceptibility of each cell may transform each cell differently, since some cells might not be directly affected by the carcinogen, but might still be altered genetically to be transformed later in their lifetime. It is believed that tumor specific mechanisms, such as genetic instability, are factors that lead to the cell heterogeneity within tumors [35]. Since cancer cells are transformed when DNA in normal cells is damaged, further errors in the DNA may lead to different types of cancer cells being transformed. DNA mutations such as point mutations, genomic rearrangements, and gene deletions give rise to phenotypic variability of cancer cells that have originated from a single cancer cell. The evidence of this comes from observing the abnormalities of karyotypes in the development of fibrosarcoma (fibroblast-derived tumor) cells that appeared to have greater mutations when they became metastatic [36]. Furthermore, studies have also shown that both genetic and epigenetic mechanisms lead to activation of repressed genes in certain tumor subpopulations [37]. [38]

Tumor heterogeneity causes variations in the growth rate, chemical production and sensitivity of cancer cells toward chemotherapy. The variation in growth was reported in study that shows how spontaneous mutations occurred mostly in metastatic subpopulations of fibrosarcoma cells [39]. Chemical production may also vary within single tumors because of the activation of repressed genes [37]. The chemical production variability may be a cause of the different levels of metastatic cancer cells in a tumor. This implies that for each different subpopulation of cancer cells, different genes coding for different proteins may be activated to support the metastatic path of the subpopulation. Chemical sensitivity of different

subpopulations of cancer cells has also been identified as a cause of tumor heterogeneity. This sensitivity has been identified to come before the transformation of cancer cells. Normal cells within tissue have different susceptibilities towards carcinogens, and as such it is believed that transformed cancer cells retain the characteristics of the normal cells that preceded them [40]. [38]

2.2.2 Effects on Cancer Treatment

Even though experiments that prove the existence of different subpopulations of cells in tumor are hard to come by, clinicians acknowledge the presence of these subpopulations. By accepting this idea, clinicians often provide explanations as to why certain drugs do not work well against a specific tumor. Tumor cell populations are believed to vary with respect to metastatic cell formation, meaning that they vary according to whether or not they can detach from the tumor tissue. Several cancer treatments' effectiveness are often stopped by the fact that metastasis has occurred in the patient. Since there are very few techniques currently available to study the composition of cancer cells while inside the tumor, clinicians often find themselves performing complicated and dangerous procedures in order to get rid of the metastasized cancer. Thus, there is a need to address tumor heterogeneity in order to identify the different kinds of cancer cell subpopulations that exist within a single tumor.

2.3 Project Significance

This project attempts to create a method that, in the long run, will allow clinicians to detect tumor heterogeneity in a fast way, by providing information of the biomolecules present within the tumors. Current techniques used in cancer treatment are very costly and do not offer a cure 100% of the times. Current techniques are also affected by the mentality of

“broad medicine” that many clinicians adopt when treating cancer patients suffering from the same cancer type. Thus, it has been decided that our project will allow clinicians to follow a personalized approach when treating patients that will let them construct cancer treatment roadmaps that will specifically focus on a single patient.

2.3.1 Current Issues

Even though cancer treatment nowadays may cause a significant improvement in cancer patients, it is true that adverse side effects and human errors often reduce the effectiveness of the cancer treatment. A study done at the University of Alabama at Birmingham provides valuable information on the amount of errors that happen in the clinical environment. The study found out that out of 20,979 patient encounters, 89 chemotherapy errors were made by the team treating the patients. Furthermore, it was found that the majority of these errors occurred due to the use of an incorrect drug or an incorrect dosage given to patient. The figure below shows the statistics obtained for this study:

Chemotherapy medication errors	37 (42%)
Incorrect drug	
Incorrect dose	
Incorrect age/dose for IT meds	
Incorrect route of administration	
Roadmap errors	23 (26%)
Supportive care errors	13 (15%)
Incorrect IV fluids	
Incorrect MESNA or dexrazoxane	
Timing errors	11 (12%)
Wrong day of administration	
Incorrect duration of medication	
Pharmacy errors	4 (4%)
Incorrect labeling	
Incorrect dispensing	
Clerical errors	1 (1%)
Incorrect identifying data (medical record number or date of birth)	

Pediatr Blood Cancer DOI 10.1002/pbc

Figure 6: Results for the study done at UAB. This is the distribution of the 89 medication errors [41].

Other issues that current cancer treatment methods have are the amount of adverse effects that the substances used cause to the cancer patients. Drugs such as Sprycel, used to treat leukemia, often have strong adverse side effects. Sprycel is known to cause pulmonary arterial hypertension, a condition that affects the heart and most often leads to heart failure. [42]

2.3.2 Personalized Approach

In order to address some of the issues that current cancer treatment methods cannot prevent, the method developed in this project is expected to help clinicians in following a personalized approach to treat cancer. There are not many technologies that allow visualization and identification of molecular composition of tumors. In order to perform personalized medicine, clinicians tend to rely on factors such the patients' age, gender, family history. There are cases however in which more specific observations on the patients' biochemistry lets clinicians make decisions. Taximofen, which is used to treat breast cancer, is used on patients who have estrogen receptor sensitivity and is not recommended to be used on patients who do not have such receptor. If any major technology allowed for the screening of the receptor's presence, then the clinicians' job would be greatly simplified. Therefore, understanding complex biological systems is essential for clinicians since this allows them to prescribe apply treatments on cancer patients without the risk of adverse effects or wasted resources. [43]

2.4 Technical Background

This project will attempt to provide a more personalized approach during cancer treatment by making a sample tumor tissue transparent while also allowing visualization and identification of proteins within the tumor sample. By making the tumor tissue transparent,

we expect to reduce light scattering and increase the deep-tissue visualization of modern imaging techniques. Proteins are a focus of our project since we also expect to provide a method to preserve proteins within tumor samples. Identifying proteins and other biomolecules in sample tumor tissue coming from a patient can potentially allow clinicians to better make decisions when prescribing a treatment for the patient. Imaging of the tissue will provide the visualization necessary for the molecules in the molecule to be identified.

2.4.1 Transparency

Optically clearing tissue allows us to match the refractive index of tissue in order to better observe the components that lie within the tissue. Several studies serve as examples of the ways in which transparency allows for deep tissue imaging. CLARITY uses a method that extracts the lipid bilayer membrane from cells to render brain cells transparent so that the cells deep within the tissue can be labeled and observed in 3D. As this study shows, transparency is achieved once the lipid bilayer membranes of cells are removed. In this project, we will attempt to perform lipid bilayer extraction using a novel approach. [8]

The lipid bilayer membrane is the outermost membrane that surrounds the human cells. Lipid bilayers are composed of phospholipids that arrange themselves in such a way that the hydrophobic ends are close to each other and the hydrophilic ends are on the outside and the inside of the cell. The lipid bilayer provides cells with structural integrity, molecular diffusion, and protection against hazardous molecules.

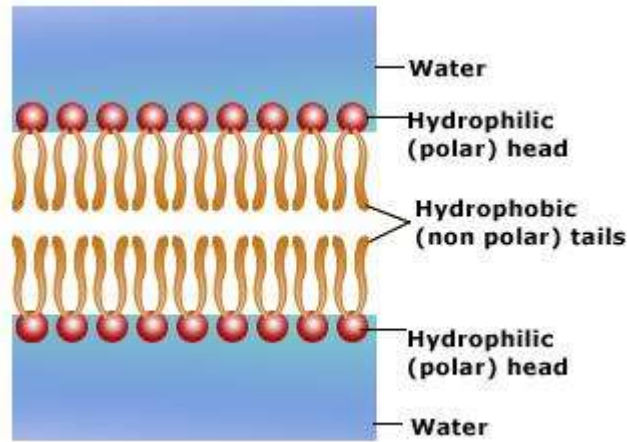


Figure 7: Lipid bilayer in human cells [44].

However, the lipid bilayer membrane is also responsible for light scattering when it comes to visualizing intracellular units. Studies show how light is scattered once it reaches the membrane of the cell, thus preventing for deep tissue imaging techniques to reach the inside of the cell. [45]

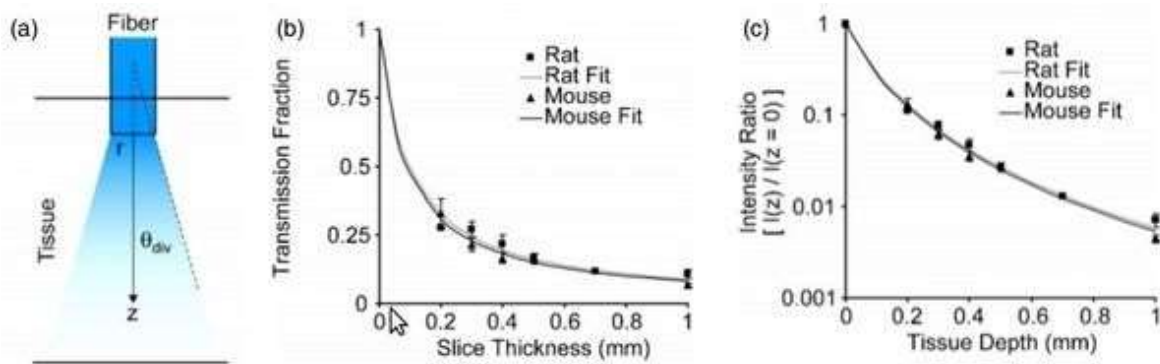


Figure 8: Transmission fraction and Intensity values of light traveling through mouse brain cells with lipid bilayer membrane [45].

The figure above shows how the transmission fraction (which refers to the amount of light that can go through a material) decreases as the slice thickness of the brain tissue increases. Also, light intensity in non-sectioned tissue tends to decrease as the depth of tissue analysis increases. This only shows how lipid membranes in human cells prevent deep tissue

molecular phenotyping. Yet, results from studies like the one shown above provide support for the idea of lipid extraction via some mechanism.

2.4.2 Proteins in Tumors

To obtain information of the biochemical composition of tumors after rendering tissue transparent, it will be necessary to label and visualize the molecules that exist within the tumor. Proteins are widely known to be active tumor biomarkers, since overexpression of certain proteins in cancer patients allow clinicians to make decision as to what treatment should be followed. In fact most tumor biomarkers can be easily obtained by taking classic tests out of the patient, such as blood or urine samples. In other cases looking for specific proteins might allow to predict the course of action that a tumor will take. A study done by researchers of the National Institute of Health and the University of Hong Kong, indicated that cancer metastasis and growth could be well predicted by measuring the protein in tumors that were surgically removed. The specific protein looked at in this study was CPE- Δ N, which is believed to form in most cancer cells once they become metastatic. Thus, the researchers concluded that by quantifying the expression of the protein it is possible to prepare techniques that can refine treatment in metastatic cancers. [46 and 47]

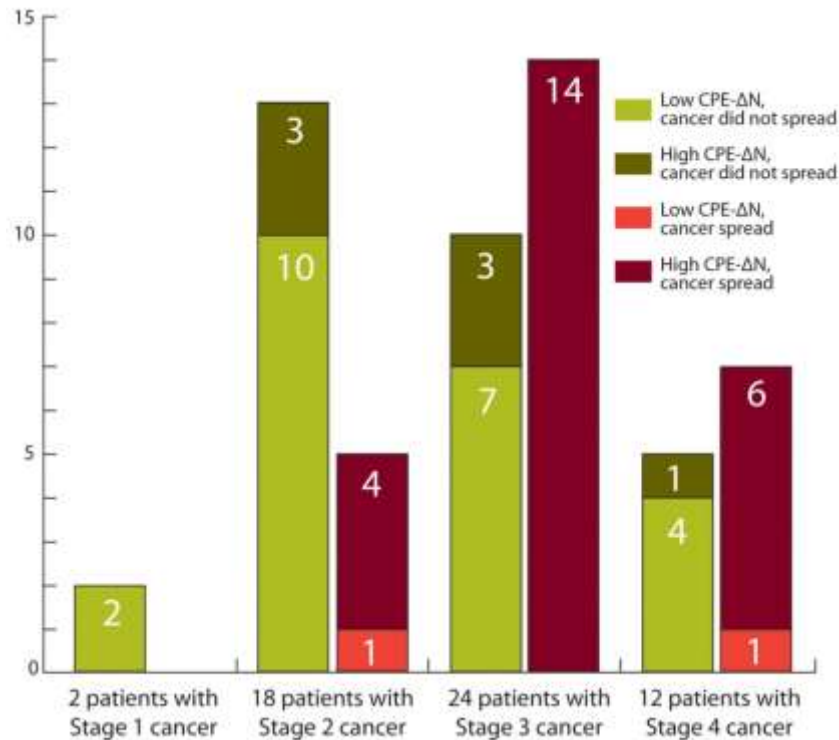


Figure 9: Results obtained in the NIH experiment. Notice how at later stages of cancer, more CPE- Δ N is found to be present in tumors [47].

2.4.3 Imaging Proteins

In order for clinicians to acknowledge the presence of a particular protein in a tumor, labeling and imaging techniques need to be used. It is necessary to be able to identify the proteins within the tissue. To do this, several methods can be performed to either directly identify proteins within tumors or to tag for fluorescent imaging. Some of the methods that are widely used to identify the presence of proteins are ELISA and immunoblotting. ELISA consists of determining if a particular protein exists within a sample. It is done by placing sample serum that has been centrifuged into the bottom of a 96-well plate. In this plate antibodies are placed on the serum containing the proteins which can then metabolize color on the wells. At the end of the procedure, optical density readings are taken to measure the amount of protein present in each well [48]. Immunoblotting consists in using gel

electrophoresis to separate proteins within a tissue extract by their 3D structure [49]. Besides identifying protein presence in tumors, labeling and imaging can be used to better visualize proteins within the tumor. By labeling proteins using specific fluorescent antibodies, it is possible to later use imaging methods such as 3D confocal microscopy or photon emission microscopy [50.]

2.5 Related Methods

2.5.1 The Cancer Genome Atlas

Currently, there are over two hundred distinct cancer types which are initiated by DNA errors which lead to uninhibited cell development. If the errors for each genome, its complete DNA set, could be monitored and studied, identifying what triggers the disease could be possible. This is a more personalized approach to studying cancer. The Cancer Genome Atlas is huge database of genome variations of cancer types and subtypes. This program was established by the National Institute of Health (NIH), The National Cancer Institute (NCI), and the National Human Genome Research Institute (NHGRI). Their goal is to create an atlas, a collection of maps, of specific cancer types. All of the data however, is open to the public. This allows researchers worldwide to contribute to this compilation and this data can also be used in research. Currently, over twenty types of human cancer has been studied and characterized. [6]

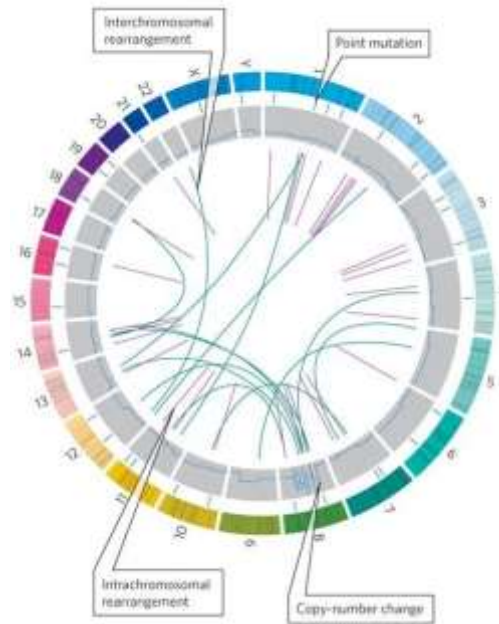


Figure 10: Circos Plot. Outer ring represents the chromosomes and Inner rings represent the locations of different types of mutations [6].

The Cancer Genome Atlas (TCGA) focuses on four main areas: Tissue Processing, Research and Discovery, Data Sharing, and Community Research and Discovery. Tissue Processing is the initial step, where a sample of tumor tissue is donated. This sample is donated along with a sample of normal tissue, most often blood. These samples, called bio-specimens, need to satisfy a strict set of standards so that the DNA and RNA can be used for analysis and sequencing. The department that handles this, the TCGA Biospecimen Core Resources, also eliminates any trace of the patient's private information. The next step, Research and Discovery, has the bio-specimens analyzed. Some characteristics studied include how gene expression occurs as well as genome rearrangement. Data Sharing occurs using this information, and it is performed by the TCGA Data Coordinating Center. The data is stored in a large public database so that researchers can search for specific cancer type information. After searching, scientists can then download and analyze the data. This leads to the final step of Community Research and Discovery, the database is open to the public so that the most up to date information on cancer genomes are being studied and sent worldwide. This personalized

approach allows a specimen from one person to contribute to a large database, where more accurate information about data can be further obtained. [6]

2.5.2 Zebrafish Study

One new technology that is making huge strides in cancer research is the use of zebrafish as an animal model of human cancer. Zebrafish develop cancer naturally and quickly and this is very useful for cancer research. The cancer is established after being exposed to a mutagen and through transgenesis, where the genetic material is being brought from a different species. One of the biggest reasons why zebrafish are being used as an animal model for human cancer is the fact that the tumors formed in a zebrafish have similar characteristics to those of human cancers. The genomes of the tumors are comparable, as well as their gene expression and their microscopic cell anatomy. The genome for the zebrafish has been fully sequenced as well. This fish can also reproduce at a frequent rate and can produce 200-300 embryos a week. Zebrafish are also an excellent model for in vivo imaging. A huge reason for this is due to the unique fact that their skin is translucent. Their skin allows us to witness tumor growth and actually see if cancer treatments are effective or not. Originally, only juvenile zebrafish were transparent, and would lose this characteristic once an adult, when it becomes opaque. However, a recent study has allowed this trait to remain when they grow into adults. [51]



Figure 11: Transparent Adult Zebrafish [51].

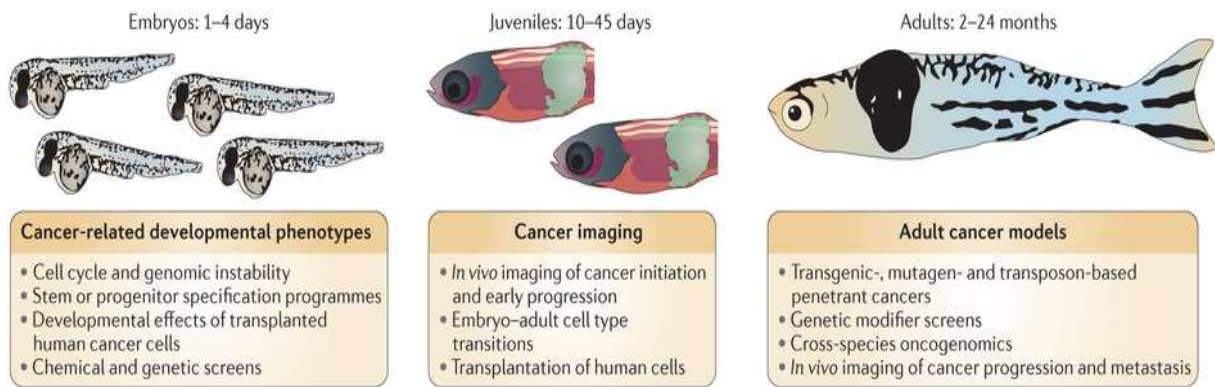


Figure 12: Advantages of Zebrafish based on its lifecycle [51].

2.5.3 Tissue on Collagen I-Hydrogel Scaffold

A huge issue in cell culture is the fact that cells grown in a 2D environment, such as in a petri dish (in vitro), is not an accurate representation of its future performance in an in vivo biological system. There has been more of an effort thought to grow cells in a 3D environment, in order to receive stimulus comparable to that inside the body. This would allow the cultured cells to acquire phenotypes, or observable traits, which would prepare it for in vivo placement. This applies to tumors as well. For this study, collage I hydrogels cultured with tumor cells was studied in vitro. [52]

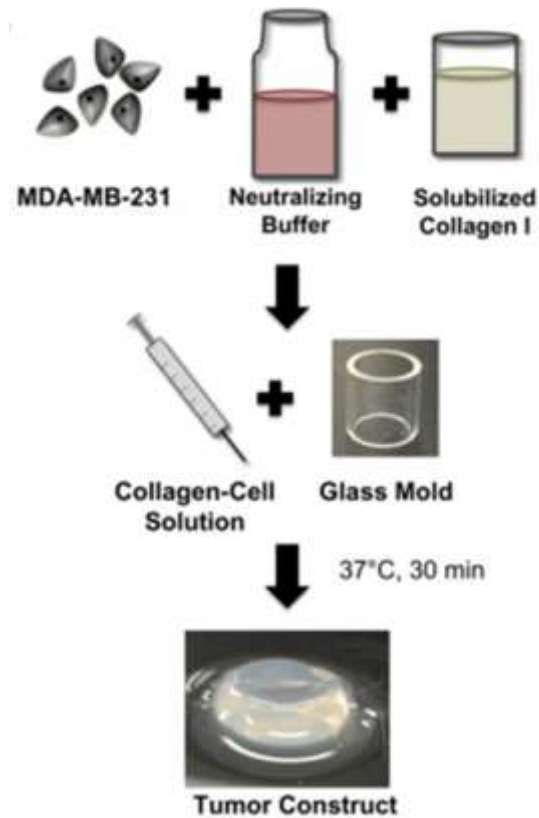


Figure 13: Collagen I hydrogel cultured with MDA-MB 231 [52].

For the cell culture, MDA-MB-231 human breast cancer cell line was used. This study mixed breast tumor cells with collagen to make a scaffold, and then studied cellular properties. The hydrogel scaffold allows for controlled observation of the tumor cells, since it fixes the proteins. It was found that cells that were cultured in collagen I hydrogels for a week established typical cell-matrix and cell to cell interactions observed in vivo. These cells also exhibited an elongated morphology which is very common for cell-matrix interactions. Once the cells began proliferating, they formed three dimensional clumps which showed the cell to cell interactions.

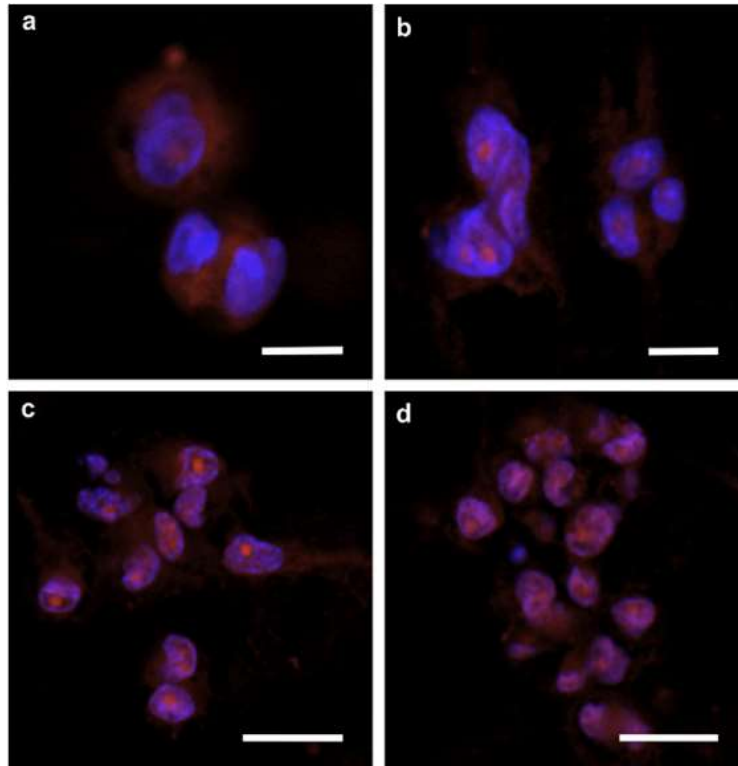


Figure 14:MDA-MB-231 cells cultured in collagen I hydrogel for a week [52].

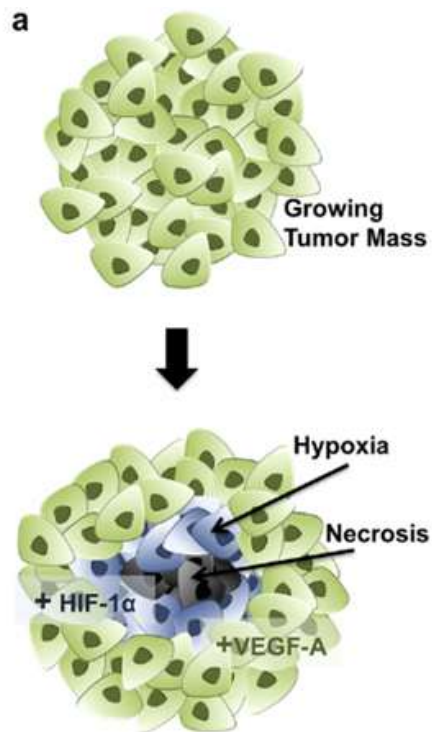


Figure 15: Tumor Necrosis due to Hypoxia [52].

This experiment had issues however. Because tumor cells were being cultured, cell proliferation was uninhibited. As cells began growing and forming three dimensional clumps, hypoxia became an issue. Hypoxia occurs to the lack of oxygen that cells towards the center of a growing tumor has. If hypoxia is not remedied, either by increasing oxygen or removing external tissue, necrosis (cell death) occurs. In order to remedy this, the group reduced the scaffold's thickness to increase the oxygen intake. [52]

2.5.4 Scale

Imaging the neurons and projections of the brain is being studied vigorously, in order to fully create and understand the structure of the brain. This has been difficult due to the issue of light scattering caused by the lipid bilayer. Scale, an aqueous reagent, is used to make biological samples optically transparent and this method allows fluorescent signals to be conserved. The reagent is used to make mouse brain and mouse embryos both transparent, and this allows the signals to be studied.

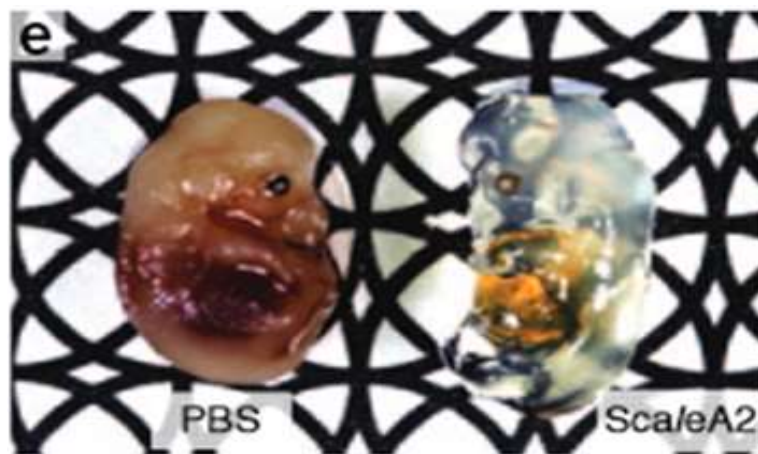


Figure 16: Two mouse embryos after fixation, left fixated in PBS and right in ScaleA2 for two weeks

This method of inducing transparency to tissue samples was first discovered by accidental observation. Polyvinylidene fluoride membranes became see-through after being soaked in 4 M urea. To further improve the transparency, the group optimized and created a solution called ScaleA2, which was composed of 4 M urea, 10% glycerol and .1% Triton X-100. This solution had to be tested, so it could be compared with other water-soluble reagents. 1.5 mm thick slices from mouse brain samples were obtained and soaked in five different solutions: PBS, 60% sucrose/PBS, FocusClear, MountClear and ScaleA2. Light transmission was determined using a spectrophotometer. The slice soaked in ScaleA2 was noticeably more permissive to visible and infrared light than the slices soaked in the other reagent.

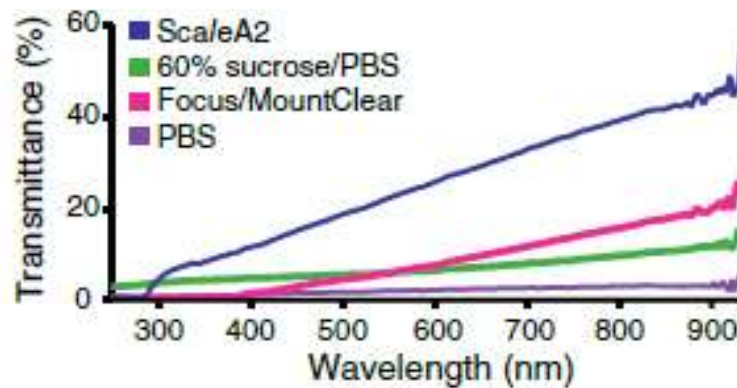


Figure 17: Light Transmittance of ScaleA2, 60% Sucrose/PBS, Focus/MountClear, and PBS [53].

Even though there was evidence for tissue swelling, after testing, it was found that the internal composition of the fixed brain kept their original proportions and form. This suggests that the tissue expansion was homogenous and uniform in every direction. Swelling is not ideal, so the group then created a new solution. ScaleU2 is composed of 4M urea, 30% glycerol and .1% Triton X-100. ScaleU2 does reduce the amount of swelling but it increases the time it takes to become transparent. Swelling affect the fragility of the cleared brain samples so this is not wanted. ScaleA2 takes a couple of days to weeks in order to make the sample translucent but ScaleU2 takes a couples of weeks to even months. Washing the ScaleA2-treated sample with PBS can shrink it back to original size.



Figure 18: Mouse brain before and after ScaleA2 (two weeks) [53].

Scale has the unique capability to preserve the signals of fluorescent proteins, while other organic solvent-based reagents removed it. Scale is also inexpensive and creating it is fairly straightforward. Because of this, Scale can be mass produced in order to clear larger tissue samples. Scale is also customizable due to the fact that its composition can be changed depending on what tissue is going to be cleared. The concentration of glycerol can be increased so that swelling does not occur as much, as in ScaleU2. Scale is also suitable for most light microscopy systems. The solution can furthermore be used for all organs. The main drawback however, being that time significantly increases for clearance. This drawback can be solved by changing the composition of the reagent nevertheless.

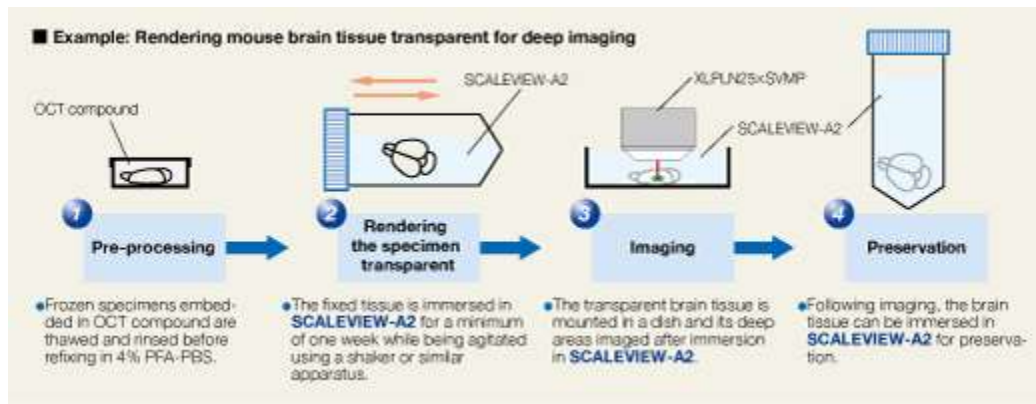


Figure 19:ScaleA2 steps for tissue transparency for deep imaging [53].

2.5.5 CLARITY

A very pertinent study was performed in Stanford University where a brain was made transparent and 3D mapped, in order to study the neural structures. Their goal was to quickly convert an intact mouse brain into a transparent and molecule-permeable brain. At the same time, basic molecular structure had to be preserved. This was an issue, because lipid bilayers on the brain, causes light scattering, thus making imaging next to impossible. The lipid bilayer has to be removed in order for light to fully penetrate tissue. This process must occur in a safe way so proteins and other material won't get denatured. Removing the lipid bilayer can affect other properties of the brain. This layer retains important molecules such as proteins which contains cellular information. The lipid membrane also supports the structure and removing this makes imaging difficult. The CLARITY (Clear, Lipid-exchanged, Anatomically Rigid, Imaging/immunostaining compatible, and Tissue hydrogel) method is used to make the brain transparent and provide a secondary support system after removing the bilayer. [8]

The initial step performed by the Stanford group was to take hydrogel monomers and formaldehyde and embed them into tissue. The hydrogel monomers, acrylamide and bisacrylamide, are used in order to create covalent bonds with important molecules such as

nucleic acids and proteins. Formaldehyde is used to crosslink the tissue at a temperature of 4°C (Figure 20). [8]

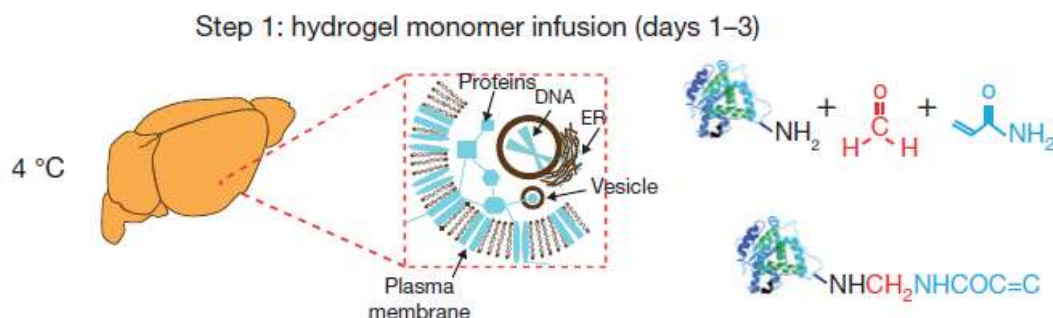


Figure 20: Infusion of monomer (blue), formaldehyde (red) and tissue.

Next, this monomer-tissue is polymerized into a hydrogel mesh by incubating at 37°C for 3 hours. The tissue and the hydrogel then become one hybrid construct and this is what will be physically supporting the tissue (Figure 21). This construct will also allow important molecules such as proteins to remain, after the lipid bilayer gets removed.

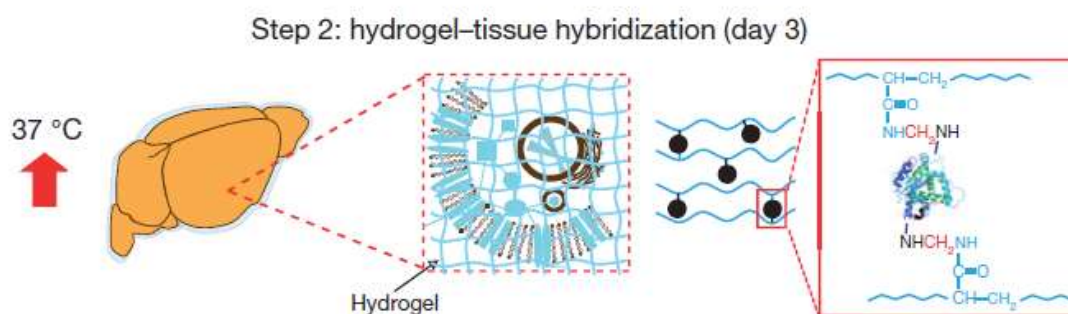


Figure 21: Creation of hydrogel mesh by incubation [8].

The third step is to get rid of the lipid bilayer. The Stanford team developed a unique ionic extraction technique in order to achieve this. This method was chosen over using a hydrophobic organic detergent because organic solvents like these quench fluorescence. These limits imaging time and this process would also take several months to clear an adult mouse brain. The team developed an active-transport organ-electrophoresis method, which

they termed Electrophoretic Tissue Clearing (ETC). This technique uses the high charged nature of ionic micelles to quickly and actively remove the lipid bilayer (Figure 22). Along with a solution, a voltage runs through an ETC chamber to remove the lipids (Figure 23). [8]

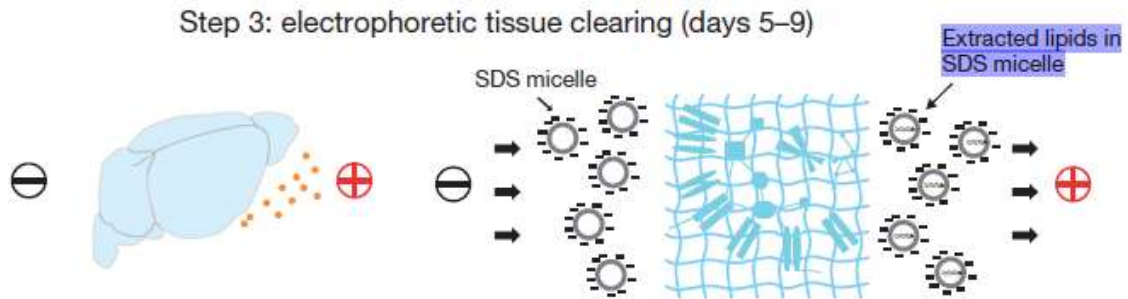


Figure 22: Removal of lipids by using SDS detergent and a voltage [8].

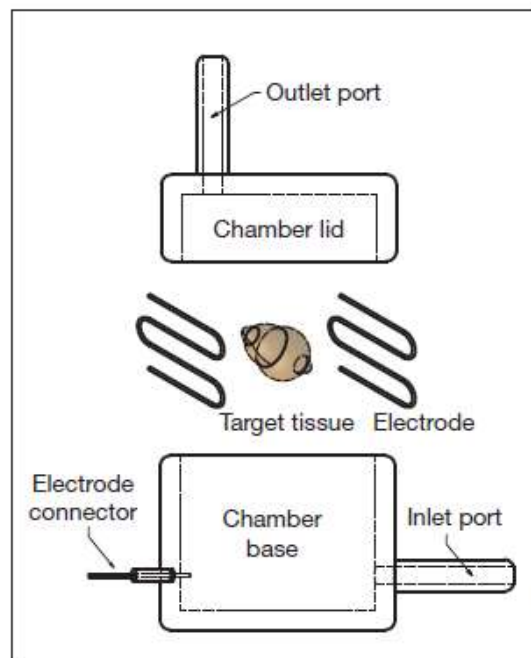


Figure 23: ETC Chamber Diagram [8].



Figure 24: Actual ETC Chamber made from Nalgene Bottle

The process took eight days to make the intact mouse brain transparent. Using single-photon microscopy, the sample was imaged and was only limited by the objective's working distance. The brain tissue did expand however there was no deformation. After imaging, protein loss of CLARITY is then compared with other reagent based methods after a week of clearing (Figure 25): paraformaldehyde (PFA) fixed tissue blocks were cleared by 4% SDS and ~65% of total protein was lost, the Scale method lost ~41% of protein, PFA-fixed tissue treated with .1% Triton X-100 in PBS buffer, lost ~24% of protein, and the CLARITY method only had ~8% protein loss. Protein loss means that it will be more difficult to image fluorescence, since the fluorescent proteins were removed.

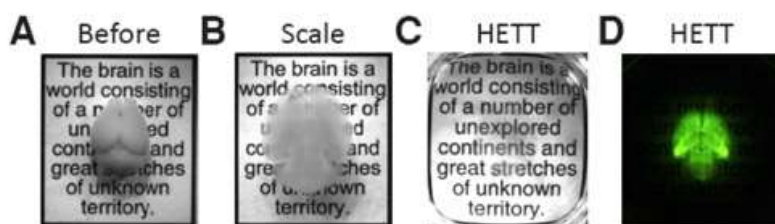


Figure 25: Images of 4 Month Old Mouse Brains. (A) Before ETC Chamber (B) Scale method for 5 weeks (C) CLARITY method for 2 days (D) Fluorescent image of C

This method is significantly faster than the Scale method. It is also better at deeply penetrating tissue. One big drawback is when the ETC chamber operates the voltage increases the temperature, which is an issue when trying to keep tissue intact.

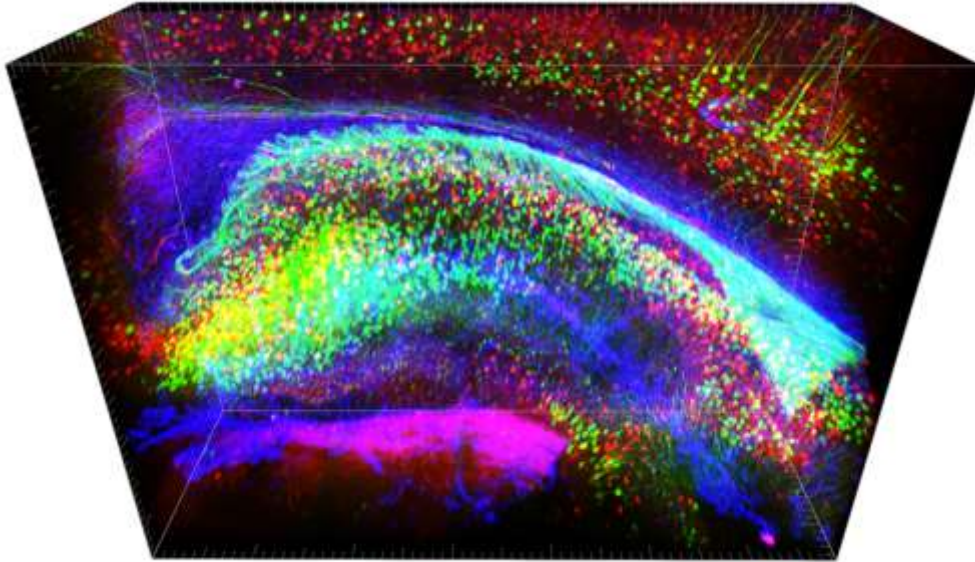


Figure 26:3D Map of Stained Hippocampus. Blue areas are supporting glia, red areas are connecting interneurons, and green areas are fluorescent-expressing neurons [8].

2.5.6 SeeDB

Another method studied using an optical clearing agent, SeeDB (See Deep Brain), also retains fluorescent proteins. Most clearing agents do not and this leads to quenching, which increases imaging difficulty. A team of Japanese scientists from the RIKEN Institute developed this agent, which is mainly made up of fructose sugar and water. By soaking the tissue sample in this solution, it will eventually become transparent due to the immersion in SeeDB. This solution has been used to get rid of the lipid bilayers of mouse brains and embryos without damaging their structural integrity. These lipid bilayers however, cause light scattering, which is the biggest issue in imaging. Light scattering is caused by a difference in refractive indexes. The refractive index of SeeDB is 1.490 which is very close to that of lipids (fats). The refractive

index using a dimensionless number indicates how well light goes through that medium (Figure 27).

$$n = \frac{c}{v},$$

Figure 27: Refractive index equation. c = speed of light in a vacuum v =speed of light in the substance [54].

SeeDB works by having the solution having a similar refractive index. By soaking in the solution, the lipids basically become see-through. SeeDB also does cause shrinkage or swelling. The only issue is that when incubated the tissue at higher temperatures, browning occurs in the fructose solution but this can be cured by adding α -thioglycerol. ScaleA2 fully cleared the adult mouse brain of lipids in 21 days, CLARITY needed 9 days, while SeeDB only takes 3 days. SeeDB also causes no change in sample volume, and is completely reversible. SeeDB is inexpensive, safe, easy, and relatively fast.

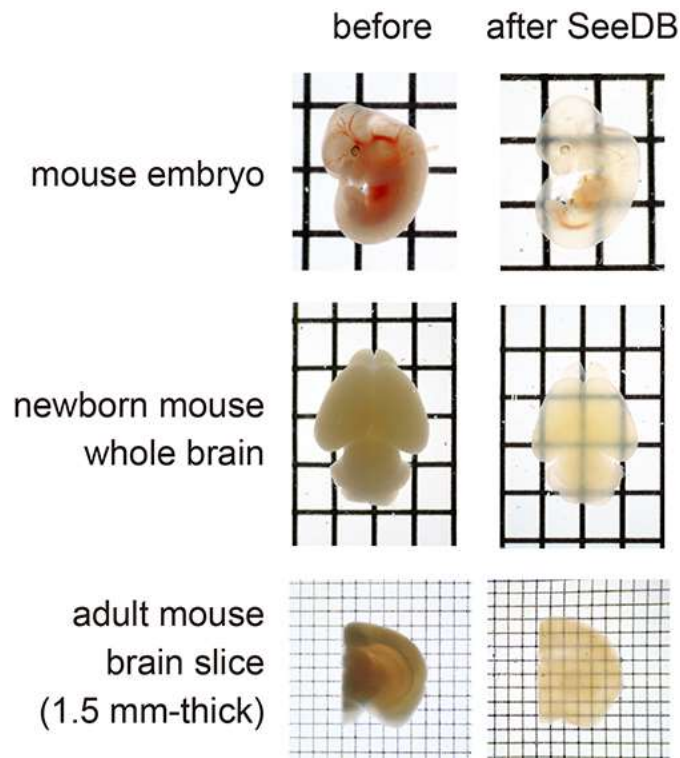


Figure 28: Various tissues before and after SeeDB [55].

2.5.7 Supercritical CO₂

Supercritical substances are fluids that are brought to a particular temperature and pressure. This particular point is referred to as its critical point, and beyond this, attains the special property of behaving like a gas and liquid (Figure 29). Supercritical fluids (SCF) can dissolve materials like a liquid while also being able to effuse through solids like a gas. [58]

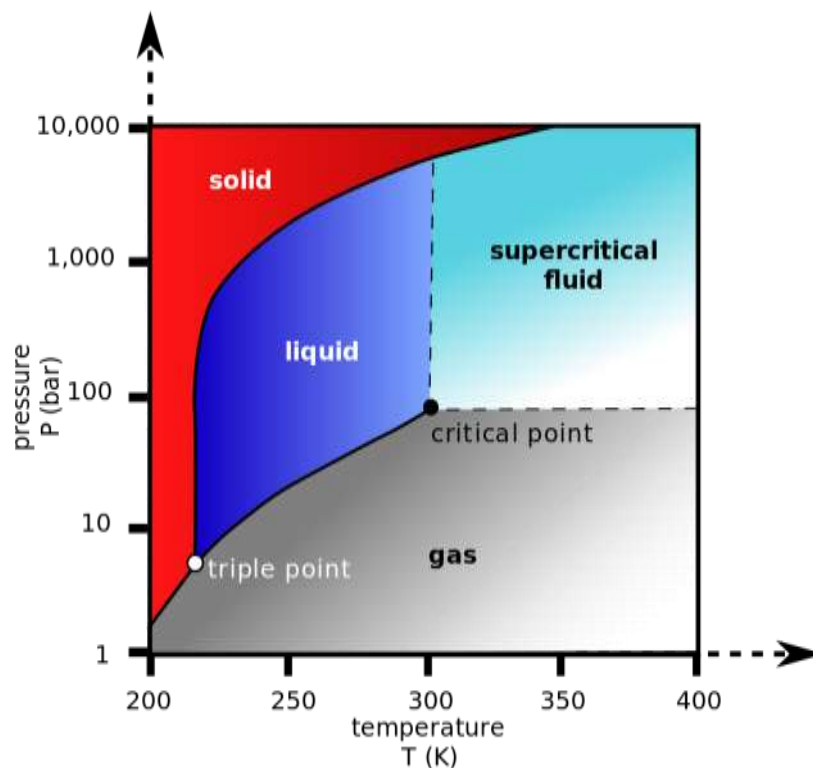


Figure 29: Phase Diagram of Carbon Dioxide (based on Pressure and Temperature) [57].

Supercritical fluids have very high diffusion coefficients and can easily remove lipids, even better than commonly used detergents. SCF also have a low viscosity so it can expand well. For example, a liquid solvent that took hours or days to extract the lipids from a tissue could take minutes if the supercritical fluid was used instead. Advantages of this technique are that it is cheap, safe, and very effective. Most organic solvents use toxic solutions, but CO₂ is not toxic in any fashion. One drawback is that not a lot of data exists on studies performed using supercritical carbon dioxide and tissues so all the effects are not readily available.

Another is that the mechanism to control temperature and pressure is more complicated than other methods.

No.	Solvent extraction	Supercritical extraction
1	Solvent presence is unavoidable. The residual level (generally ppm) of the solvent depends on the type of solvent used	Is totally free of solvents and hence very pure
2	Heavy metal content is also unavoidable and depends on the solvent, the method of solvent recycling, the source of the raw material, and the material used to construct the contact parts of the machinery	Totally free of heavy metals since they are not extractable even if they are present in the raw material. No heavy metals are present in CO ₂ or the equipment
3	Inorganic salt content cannot be avoided, using the same concept as above	Totally free of inorganic salts using the same explanation as above
4	Polar substances get dissolved along with the lipophilic substances from the raw material due to poor selectivity of the solvent. During solvent removal operations, these polar substances form polymers, which lead to discoloration of the extract and poor flow characteristics. All this causes the extract to look different from the basic components in the raw material and hence it is more of a "pseudo" natural extract	No such possibility exists since CO ₂ is highly selective and no chance of polar substances forming polymers exists. In addition the operating temperature is only 40–80 °C
5	Both polar and non-polar colours are extracted	Only non-polar colours get extracted
6	Solvent removal requires extra unit operations resulting in higher cost and lower recovery of useful material	No extra unit operations needed and yield of useful material is very high

Figure 30: Comparison of supercritical extraction and solvent extraction [58].

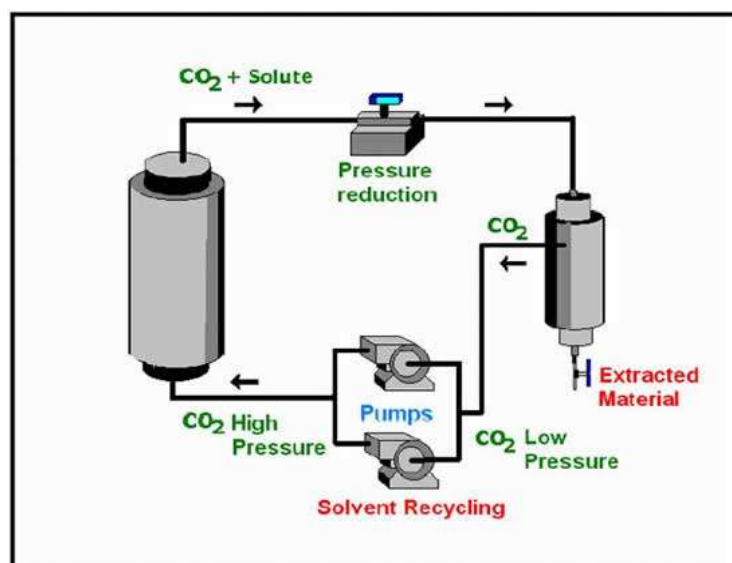


Figure 31: Supercritical Fluid Extraction Diagram [58].

Chapter 3

Project Strategy

3.1 Initial Client Statement

The initial client statement provided by the project advisor, Dr. Ming Su, informed the group of the possible improvements for cancer therapy, assuming the project is successful. The group then organized a detailed literature review in order to understand present shortcomings and current products based on the given statement. While expanding our knowledge on the issue, the team took note of possible objectives and constraints for the project design. After further discussions with the project advisor, who was the client as well, the team created a list of functions that the design had to fulfill. This culminated with a revised and focused client statement.

The original statement conveyed by the project advisor, Dr. Ming Su, was: "Tumor is a heterogeneous construct. Assessing tumor heterogeneity as part of a diagnostic may help to better predict a patient's potential for response, and provide rationale and selection of therapy. This project is to develop a method that allows 3D fluorescence technique to check tumor heterogeneity in tissue by making this tissue transparent to visible light. A hydrogel scaffold will be generated by ultrasound enhanced diffusion of hydrogel pre-polymer into tissue, radiation induced polymerization of pre-polymers, and electrical leaching of non-transparent lipids. A variety of fluorescence molecular probes will be used to label tumor specific proteins, and provide a 3D map of how tumor cells and normal cells are arranged in a heterogamous environment."

3.2 Objectives

After conducting more research, it became apparent to the group what key characteristics the final design would need in order to be successful. Key objectives were discussed with the client, until a list of six core objectives was created. The final design will be adaptable, fast, inexpensive, reliable, safe, and user-friendly.

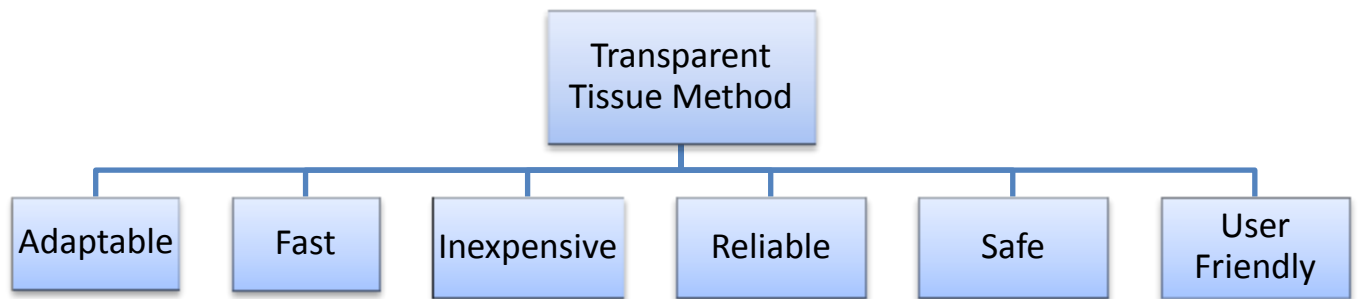


Figure 32: Objectives Tree

For assessment purposes, a pairwise comparison chart was produced, as seen below in

Table1:

	Inexpensive	Adaptable	Reliable	Fast	Safe	User Friendly	Total
Inexpensive		0	0	0	0	0	0
Adaptable	1		0	0	1	0	1
Reliable	1	1		0	1	1	4
Fast	1	1	1		1	1	5
Safe	1	1	0	0		0	2
User Friendly	1	1	0	0	1		3

Table 1: Pairwise Comparison Chart

The most important was the “Fast” objective. The two current methods researched, CLARITY and Scale, took weeks to fully finish the 3D mapping, even though most of the time was spent waiting for the tissue to become transparent. This length of time is not acceptable, because it takes too long for a tumor sample to be tested, and this would lead to a delay in therapeutic use, regarding what drug should be given to combat the cancer. The second most important objective was for the design to be reliable. The process of preparing transparent tissue samples has to work every single time. If our design was used in clinical applications any errors would cause clinicians to give incorrect advice and thus have the patient suffer from drug’s side effects. The process must not be overly complicated as well. The third most important objective was that the process has to be user-friendly. We do not want the process to be limited to only very technical positions. The fourth most important objective is that the method is safe. This means that the toxicity of the reagent used has to be minimized. The method of creating the transparent tissue needs to present no hazards as well. The fifth most important objective was that it has to be adaptable. The Scale method has the drawback of tissue becoming swollen due to the long amounts of time of being immersed in solution. The CLARITY method had the drawback of having the electrophoretic tissue clearing chamber becoming warmer as current ran through it. Our design should be able to adapt to these changes and provide a counter measure to ensure proper data will be obtained. The least important and last objective is that the process has to be inexpensive. Some materials in the process must last long enough to be reused. The design has to be relatively cheap to build and, further down the line, cheap to run/repair.

3.3 Constraints

Subsequently discussing the objectives with the project advisor, several constraints were created in order to shape the design process. The cost of the final design cannot exceed \$212 because of our project's budget constraint. The tissue samples that we use to test our design on will be obtained from the laboratory itself and will not be purchased. Another constraint is time; the team only has until May 1, 2014 for submission of e-CDR. The group also needs to create a method that takes a shorter amount of time than the two weeks that it took Scale/CLARITY. Two big constraints that are vital to the design are temperature and pH. Temperature needs to remain constant at 37° C. The pH also needs to be regulated, between 6.5 and 7.5. Outside this range, irreversible damage will occur to the tissue-hydrogel construct. When making the tumor tissue transparent, the voltage that runs through the electrophoretic tissue clearing chamber would cause the temperature to rise. This needs to be limited because it would degrade the tissue sample. For pH, cancerous tissue has a lower pH than regular tissue, so adjustments will need to be made, for the varying ranges in pH, for the solution.

3.4 Revised Client Statement

Develop a cost-effective, time-effective and replicable method that enables tissue transparency by supercritical fluid extraction. This method should provide reliable results quickly, maintain structural integrity of the tissue after extraction, exhibit improvement in tissue transparency, and minimize toxic byproducts. This method should provide the foundation for a future scalable extraction chamber for tissue samples with the goal of allowing clinicians to determine and analyze tumor heterogeneity by imaging transparent tissue.

3.5 Project Approach

3.5.1 Technical Approach

The first step in creating the design was selecting a hydrogel that would preserve the tissue, no matter what stresses occurred to it. Research was performed and hydrogels were examined, with the goal of only binding to protein and nucleic acids, and not lipids. These lipids need to be extracted and our design had to be extremely efficient, in order to improve the biggest drawbacks of current clearing technologies: time. By studying the three different clearing methods, a unique method is obligatory in order to satisfy the clearing speed. Testing will also be performed prior to tissue experimentation, in order to quantify the procedure.

3.5.2 Design Evaluation Matrix

A design evaluation matrix was made in order to determine the viability of potential design alternatives. The alternative designs needed to meet the following constraints: time (about six hours), final cost (less than \$212), and temperature/pH/pressure adjustment. The objectives which served to compare the alternatives were: fast, inexpensive, user-friendly, reliable, safe, and adaptable. A scale from 0-50 was used to compare how well objectives will be met among the three preliminary alternatives.

Design Constraints (C) and Objectives (O)	ETC Chamber	Supercritical CO₂	Optical clearing reagent
Time "<6 hours" (C)	no	yes	no
Cost "\$212" (C)	yes	yes	no
Adjustable (C)	yes	yes	yes
Fast (O)	40	50	20
Inexpensive (O)	30	50	20
User-friendly (O)	20	30	50
Reliable (O)	45	40	20

Safe (O)	10	50	15
Adaptable (O)	20	30	50
Total score	165	260	175

Table 2: Design Evaluation Matrix

Based on the total score obtained in the design evaluation matrix, our most favorable preliminary design involves the use of supercritical CO₂.

3.5.3 Design Functions and Specifications

Based on literary research and comprehension of our objectives and client statement, the team focused on forming an inclusive list of functions and specifications for our design.

3.5.3.1 Functions

For the establishment of functions, the team created a list of tasks that the device must be able to do:

Function 1: The device must not damage tissue.

Function 2: The device must not cause degradation of hydrogel.

Function 3: The device must remove lipids quickly.

Function 4: The device must contain a solvent.

Function 5: The device must allow removal of byproducts after lipid extraction.

Function 6: The device must maintain a minimum temperature.

Function 7: The device must maintain a constant pH.

3.5.3.2 Specifications

Using the functions list as a model, the team created customized specifications for the design. The constraints that limit the team are time, budget, pH of tissue, and temperature of tissue environment. Based off of these constraints, and adding into account the objectives and functions, the team established specifications for the device, which are shown below. This list was created to satisfy the specific design needs:

- Control pH of hydrogel and tissue in the range of 6.5 to 7.5
- Produce environment with a maximum temperature of about 37°C
- Maintain original tissue structure after lipid removal
- Take a maximum of 6 hours to remove lipids
- Yields a 10% transparency improvement

Chapter 4

Alternative Designs

4.1 Needs Analysis

Our team created a list of the needs that the final design needs to cover. To do this, our team looked back at the revised client statement. The client statement allowed us to identify that our design needed to be time-effective, replicable and efficient. To further clarify the needs of our design, our team met on a weekly basis. In these meetings, the team discussed the different possible final designs of the project. During these meetings the team came up with the list of objectives, constraints, functions, and specifications that were listed in Chapter 3. Our team then created a Needs Analysis Chart to establish the guidelines that the final design had to follow to ease the process of final design selection. The Needs listed on such chart are meant to demonstrate the qualities that the final design needs to have in order to satisfy our team's objectives and constraints. The Wants listed on the chart represent all the desired qualities of our final design. The Wants are not considered to be a vital part in the final design and can thus be absent from a design choice. The following table shows the Needs and Wants used for our design analysis. It also provides a brief description of each Need and Want.

Needs	Definition
Adaptable	The ability of the design to hold different tissue sizes and types (in terms of weight, volume, and composition).
Accurate	The ability of the design to yield accurate results (in terms of transparency limit).
Time-effective	The ability of the design to perform under a specified time limit.
Safe	The ability of the design to effectively reduce waste material production, to reduce potential hazards inherent to the design itself, and to reduce hazards related to handling of the device.
Ease of use	The ability of the device to be handled with ease. This also refers to the ease in test reproducibility.

Wants	Definition
Self-regulation	The ability of the design to regulate solvent flow and inherent design properties (such as temperature, pressure, and pH).
Manufacturability	The ability of the design to be easily manufactured and reproduced.

Table 3: Defined Needs and Wants table

The needs of our design correspond to what the team considers to be the most important characteristics of a functional system. For the first two Needs, “Adaptable” and “Accurate”, our team valued the idea that the design must yield accurate results. For this to happen, the design needed to adapt to the different sizes of tissue samples that were collected for testing. The “Accurate” Need told us that the design needed to yield accurate results. This implies that the transparency achieved after lipid extraction must be sufficient to be noticed by the naked eye.

The remaining Needs of our design, “Time-Effectiveness” and “Safety”, focus on particular aspects of the design instead of focusing on the end goal of the design. The “Time-Effectiveness” Need was based off of our constraint that the final system must perform under six hours. The need to have a safe system takes into account the fact that the lipid extraction device should work under minor hazardous conditions. The device needs to work under temperatures and pressures that might cause threats if the device is mishandled. Thus, it was important to prepare a device that could sustain relatively high temperatures and high pressures without presenting much of a hazard to the user. Also, the device must need to provide a safe way to get rid of waste products that may arise from the lipid extraction. In the best case scenario, the design should reduce toxic waste to zero. The Need “Ease of Use” refers to the lack of complexity involved in handling the device. This Need will allow us to determine the level of difficulty in operating the final device once it has been built. Ideally, the device will not provide a challenge while it is being handled or while the tests are done.

The Wants of our design refer to the characteristics that the team desired to include in the final device. However, the Wants are not essential for the final device to be considered a success. Instead, the wants for this design are characteristics that under ideal conditions will be included in the design. The wants for this design are “Self-Regulation” and “Manufacturability” and are shown in Table 3. The “Self-Regulation” Want focuses on the way in which the system, specifically the lipid extraction device, will regulate solvents and other properties such as temperature and pH. The “Manufacturability” want refers to the ease of fabrication of the device as well as the ease of assembling. It is desired for the device to be manufactured using materials that are both inexpensive and readily available.

4.2 Conceptual Designs

In order to create a device with the required functions, objectives, specifications, and constraints, multiple preliminary design proposals were created. Because the two main tasks of the design involved the hydrogel and supercritical fluid extraction (SFE) apparatus, achieving those tasks became the focus for the conceptual designs. Achievable methods for lipid extraction involve the use of a clearing agent, electrical leaching, or supercritical CO₂ and all three methods can use hydrogel without any issue.

4.2.1 Clearing Agent as a Solvent

The first conceptual design was based on solvent use. Aqueous reagents are often used to make biological samples optically transparent and this method allows fluorescent signals to be conserved. By observing studies such as Scale and SeeDB, it was determined that fructose and urea are methods of extracting lipids. SDS tissue clearance is also another popular method. All in all, these detergents are used to bind to hydrophobic surfaces to extract lipids

within tissues. We also proposed a hydrogel system to be used alongside the solvent to bind to proteins and nucleic acids and help maintain tissue structure. After the tissue is embedded in the hydrogel, immersion into the clearing agent is next. The clearing agent, SDS, Scale, or SeeDB, will only remove lipids, because the hydrogel is bound to protein and nucleic acids, thus preserving them. This conceptual method is the simplest, only requiring immersion into the solution, and removal of sample after certain amount of time.

4.2.2 Optical Clearing through Electrical leaching

The second concept was based off of Stanford's CLARITY. A chamber was built based off of electrophoretic technology. Electrophoresis is based off of separating molecules through the use of an electric field. This method would use the high charged nature of ionic micelles to quickly and actively remove the lipid bilayer membrane of cells, with a voltage running through an ETC (Electrophoretic Tissue Clearance) chamber. The chamber would also be inside an ice bath to help minimize tissue damage caused by the temperature increased due to voltage. Our design would be based off of CLARITY and would be improved by incorporating a pump that circulates optical clearing solution and filters out extracted lipids. The design would also have a mechanism to decrease the temperature increase caused by the voltage, and this would enable a higher voltage in order to increase the clearance speed without the drawback of tissue damage due to heat.

4.2.3 Supercritical CO₂ for lipid extraction

The last concept is based off a current method of creating perfumes, soaps, and other cosmetics []. Supercritical fluids such as CO₂ have been used in fruits industries to extract oils from fruits and plants. This method would utilize the high diffusivity and low density of

supercritical CO₂ to only remove the lipids from the tissue. A chamber would be created that incorporates a pump system, a cooler, and an oven. The CO₂ would flow from the carbon dioxide tank and go through the cooler, and then be pumped into the oven, where it becomes supercritical due to the increase in temperature and pressure. This method is very complicated due to the numerous contraptions needed to extract the lipids from the tissue. The method itself shows promise in the fastest lipid extraction, and so this was the model for our design. However, due to the complexity of the SFE mechanisms that currently exist in industry, alternative methods for creating a supercritical fluid were explored. We found out that there were less complicated methods for producing supercritical fluids, and so we based our modeling off of one of those methods.

4.3 Design Modeling

Modeling was done in order to visualize the chosen concept for the design. Computer software (Solidworks) was used to create a 3D model of what would later be the design schematic for a real life prototype. The computer model was based off of an engineering model created by Krasnow for the purpose of oil extraction from various natural products (coffee, vanilla, and cinnamon) [60]. Its main components were the upper CO₂ chamber and the lower extraction chamber. Two caps secured the upper chamber, while one of those caps had a pressure gauge attached to it. Two endplates were attached to the extraction chamber. The lower endplate had an O-ring in order to prevent CO₂ from escaping at the connection between the lower endplate and the extraction chamber. Four bolts and four nuts were used to hold the endplates in their place. A valve was connected to the lower cap of the CO₂ chamber to the upper endplate of the extraction chamber. A second valve was connected to the lower endplate. The figures below show the CAD models of the SFE chamber we created at the beginning of the project.



Figure 33: CAD model of the supercritical fluid extraction chamber.

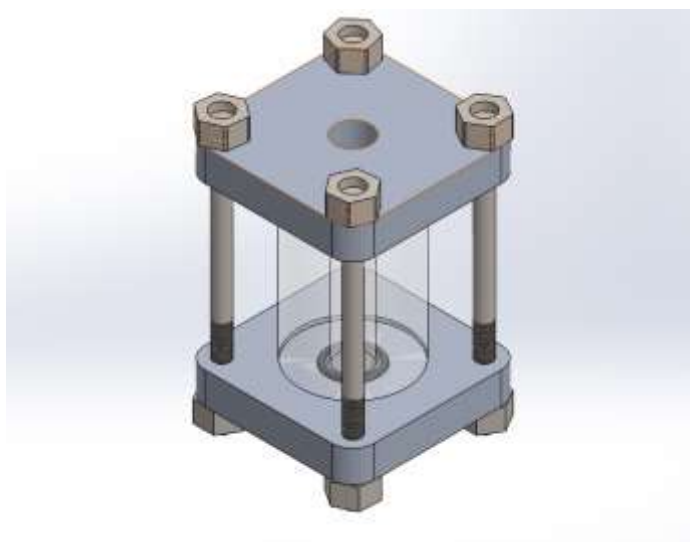


Figure 34: CAD model of the lower extraction chamber.

After creating the CAD model of the design that the team chose for the SFE chamber, the team decided to purchase the materials needed for the SFE chamber from McMaster-Carr. The CAD model allowed us to adjust the dimensions of the chamber based on the model developed by Krasnow and the needs of our design outlined in the Needs Analysis Section [60]. Below is a list of all the materials we required to build the initial SFE chamber:

Item	Specification
Acrylic column	2.50" x 4.00" (OD x H) 3/4" (center hole)
Aluminum endplates	4" x 4" x 3/4" (L x W x H) 3/8" (bolt hole D) 1/2" (center hole D) 2.50" (o-ring OD)
Schedule 80 steel pipe nipple	3.00" x 10.00" (D x H) 2.25" (hole D) External thread
Steel caps	3.50" x 2.00" (D x H) 3.00" (hole for pipe D) 1/2" (hole for valve D) 1/4" (hole for pressure gauge) Internal thread
3/8" Bolts	1/2" (Side of hexagonal head) 3/8" x 6.00" (D x H) External thread
Nuts for 3/8" bolts	1/2" (Side of hexagonal head) 1/2" (H) 3/8" (center hole D)
Valves	1/2" (OD) External Thread
Pressure gauge	1/4" (OD) External thread
O-ring	15/16" (ID) 1 3/16" (OD)

Table 4: Specification table for the materials used to build the SFE chamber.

In addition to the materials used for the SFE chamber, a few other materials let us put the SFE chamber together and run the extraction. Military grade tape was used to prevent leaks. A blowtorch using propylene as its fuel was used to heat up the upper CO₂ chamber. Heating tape was used on the bottom valve to maintain heat as CO₂ escaped through that valve. A wrench was used to tighten connections, whereas a small duty vise was used to hold the entire chamber onto a table.

4.4 Feasibility Study

Once the prototype SFE chamber was built, a few tests were done to ensure that it would meet most of the needs developed in the Needs Analysis section. These tests were done to assess that the SFE chamber was capable of keeping CO₂ beyond its supercritical properties and to assess the lipid extraction device's ability to properly extract lipids.

First of all, we assessed for proper assembly and leaking. To do this, the team assembled the SFE chamber for the first time as shown Figure 35. In order to see if the chamber could reach the supercritical CO₂ minimum pressure, dry ice was packed inside the CO₂ steel chamber. This chamber was then heated with the blowtorch until the pressure needle on the pressure gauge went past 1100 psi. Since thermocouples were not available in this project, temperature readings were done by attaching an instant-read needle thermometer to the side of the CO₂ chamber. In order to check for potential leaks at the different connections of the entire SFE chamber, we identified leaks using our fingers to feel for escaping gas. Plus, the condensate of water that formed as air hit the chamber helped us see the leaks as bubbles formed when the water droplets hit the connections of the chamber.



Figure 35: Assembly of the SFE chamber.

Second, we did another feasibility test to determine if our SFE chamber was capable of extracting oils from fruits. From our research we found that SFE on fruits such as oranges or vanilla yields oils that vary in quantity based on the pressure and temperature conditions used in the extraction. The setup for our extraction was also based on Krasnow's setup [60]. The setup consisted on placing dry ice in the CO₂ chamber, sealing the chamber, and heating it up until the pressure was above 1100 psi. At a certain point, the temperature was also measured to make sure that it had gone beyond the critical temperature of CO₂. Prior to heating the chamber, the fruit samples were cut in small pieces and were put in the extraction chamber. Having placed the sample in the extraction chamber, we proceeded into heating the CO₂ chamber. After the temperature and pressure had reached the critical properties of CO₂, we opened the lower valve. A small glass beaker helped us collect the extract we obtained

from the samples. It is important to note that there was an adjustment made after the vanilla samples were used. The acrylic used for our extraction chamber was very prone to being dissolved by the supercritical CO₂. So, after we opened the upper valve on the extraction chamber for one of our extraction tests, the acrylic chamber burst. This made us change the way in which we did future extractions. From then on, the orange samples were placed in the CO₂ chamber along with the dry ice until we decided to start testing SFE on tissue.

To determine the identity of our extract we used a UV-Vis spectrophotometer technique. From our literature, we found the absorbance properties of limonene (orange oil's industrial name). We set the baseline in the spectrophotometer using dH₂O. We then mixed some of our orange extract with dH₂O, placed this solution into a cuvette and then into the spectrophotometer slot. The cover of the device was closed and the software was set for the analysis. The software of the spectrophotometer was set up to take absorbance values between 200nm and 340nm. After making sure that all was in place, we ran the spectrophotometer. The resulting absorbance values are presented in the next section.

4.4.1 Preliminary Data

Our preliminary data was obtained after assessing the capacity of our SFE chamber to extract oils from fruits while maintaining CO₂ in its supercritical state. For our assembly tests, we assessed whether or not our chamber could reach the supercritical properties of CO₂. For our extraction tests, we attempted to collect oils from the fruit samples in order to determine if our design was capable of extracting lipids from fruits.

There were several observations made for the SFE chamber assembly after loading it with CO₂. First of all, the SFE chamber did allow for the CO₂ to go to a supercritical state. For all the extractions, the temperatures reported were between 31°C and 40°C. Unlike the

temperatures, the pressures varied for each extraction. For the extraction using vanilla samples, the highest pressure that the SFE chamber reached was 1100 psi. Rupture of the acrylic chamber occurred at that pressure. For the subsequent extraction using orange samples, the pressure went as high as 1400 psi. Leaking always seemed to occur but with varying degrees. The most leaking occurred at the connection between the lower cap and the CO₂ chamber.

As for the extraction of oils from the fruits, there were several results obtained after doing extractions. For the vanilla samples, there was a little amount of extract collected and so no analysis was done over that extract. For the orange samples, a considerable amount of extract was obtained in the order of about 5mL-10mL. In order to analyze the composition of this extract, we collected the sample and did UV-Vis spectrophotometry analysis on it to take absorbance values and compare them to the known values of limonene.

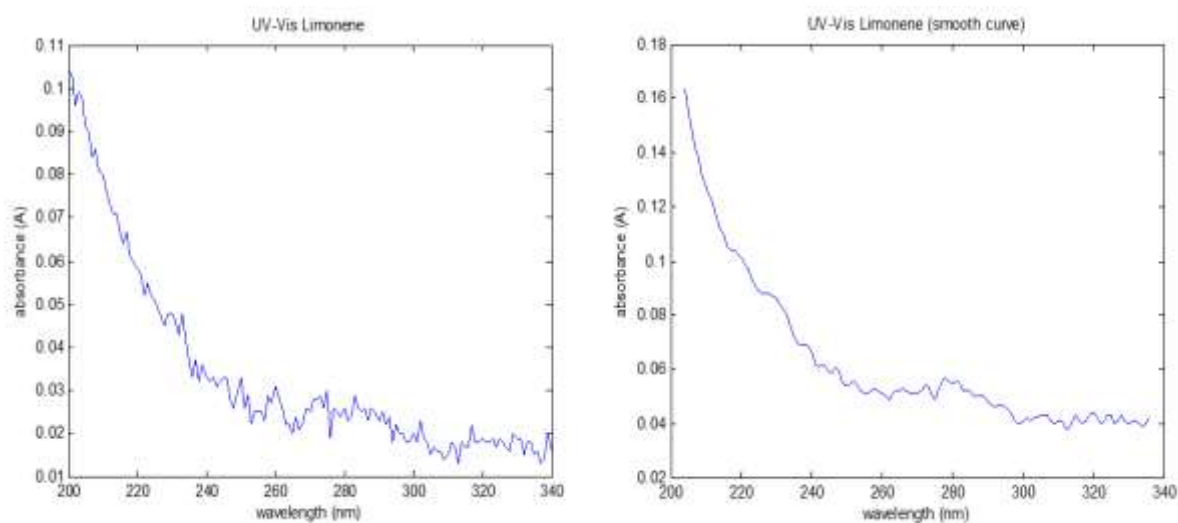


Figure 36: UV-Vis absorbance spectra of the extract obtained from the orange samples. The original absorbance plot is on the left, while the smoothed absorbance plot is on the right.

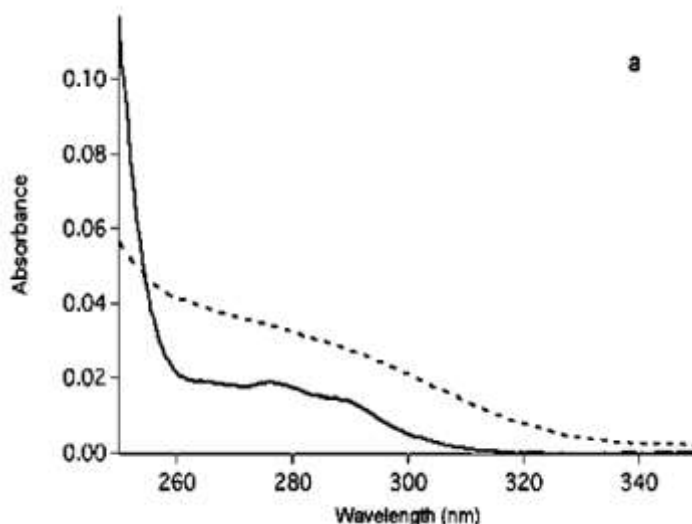


Figure 37: UV-Vis spectra of the reference limonene.

As illustrated in Figures 36 and 37, the UV-Vis absorbance values of the sample appeared very similar to the known values of limonene. The differences between our UV-Vis values and those from the reference limonene are due to (1) the wavelength used to measure the absorbance values for our sample, and (2) possible impurities that were in our extract.

4.5 Final Design

The final design for a SFE chamber device chosen by the team consisted of the following main components: a CO₂ chamber, an extraction chamber, valves to regulate flow, a thermometer and a pressure gauge, and a heat source in the form of a blowtorch. The CO₂ chamber was made of a Schedule 160 steel pipe after determining that the maximum pressure of the previous Schedule 80 steel pipe remained unknown after contacting the suppliers. The Schedule 160 steel pipe is known to support pressures up to 3000 psi in room temperature and was thus a safer choice. Two high density steel caps were tightened at the end of the steel pipe to seal the chamber. The extraction chamber was changed from the acrylic one to a stronger aluminum chamber. The extraction chamber was held by two aluminum endplates

which were held by four bolts and four nuts. Valves were placed on the connections between the CO₂ chamber's lower cap and the extraction chamber's upper endplate, and on the extraction chamber's lower endplate. The SFE chamber thus allowed for a blowtorch to heat up the CO₂ chamber until CO₂ became supercritical. The valves then regulated the flow of supercritical CO₂ from the CO₂ chamber into the extraction chamber and from the extraction chamber into a glass beaker. All of the final design's components and their specific dimensions and properties are shown in the Appendix.

Chapter 5

Methodology (Design Validation)

After assessing the properties of our preliminary design through our feasibility tests, we decided that the concept of SFE was feasible to be used for lipid extraction in tissues. Furthermore, we also managed to design a SFE chamber that extracted oils from fruits. These preliminary results gave us proof that SFE using CO₂ was going to prove useful in extracting lipids from tissue. Thus, our team decided to prepare a set of procedures in order to test our design's efficiency in removing lipids from tissue. Just as with the initial design, we decided to do extractions while measuring the temperature and pressure on the CO₂ chamber to determine if supercritical conditions for CO₂ were met. We also decided to incorporate a hydrogel scaffold into our design in order to maintain tissue integrity while undergoing extraction. We decided to do this because of the potential of high pressures in the chamber to damage the tissue. Finally, after running several extractions we decided to assess changes in transparency in tissue by observing them against a patterned background. As will be later explained, this was done to observe the differences between tissue samples prior the extraction and tissue samples after extraction.

5.1 SFE Chamber

Asides from the materials previously used in the feasibility tests, a new set of materials were needed for tissue lipid extraction. After looking at the results from the feasibility tests, the team identified a few changes to be made to the SFE chamber in order to extract lipids from tissues effectively. From our previous tests, we knew that the acrylic chamber had to be substituted for a stronger material that could resist higher pressures for a longer period of time. We decided to purchase an aluminum rod, machine it, and use it as our extraction chamber because of its stronger temperature and pressure properties. Once the aluminum chamber was incorporated into our SFE chamber assembly, we obtained the tissue that was going to undergo the extraction. We acquired porcine liver tissue and cut it to sizes

small enough that allowed us to put them into the aluminum extraction chamber. As we did extractions, we determined that varying tissue sizes would allow us to obtain more or less extract. For this reason we decided to cut tissues with thicknesses ranging from 5 mm to 1.5 cm.

5.2 Hydrogel Scaffold

The porcine liver tissues were embedded on a hydrogel scaffold that would maintain integrity of tissues as supercritical CO₂ extraction occurred. The complete protocol of hydrogel preparation can be seen on the Appendix. Briefly, 100mL of a Hydrogel Monomer Solution consisting of 4% Acrylamide, 0.05% Bisacrylamide, 0.25% VA-044 Initiator, 16% PFA, 1X PBS, and dH₂O was prepared and stored at -20°C. The liver tissue was then placed into the solution. The tissue-hydrogel solution complex was then incubated at 4°C for 2 days to allow diffusion of the hydrogel solution into the tissue. After incubation, the hydrogel solution was degassed to replace oxygen with nitrogen. Next the tissue was incubated at 37°C for three hours. After this period had passed, the hydrogel polymerized and formed a gel. The tissue-hydrogel samples were then extracted from the gel. These samples were then washed with a Clearing Solution made of 200mM Boric Acid, 4% SDS, and dH₂O for 24 hours. This was repeated two times before the samples were taken out and prepared for extraction. [61]

5.3 Supercritical Fluid Extraction Setup

The team used various unique tests in order to measure the reliability of the device in comparison to the methods of CLARITY, Scale, and SeeDB. Three tests were performed and they were:

- Pressure testing: to determine if the supercritical pressure of 1071 psi was reached.
- Temperature testing: to determine if supercritical temperature of 31°C was reached.
- Leakage testing: to determine that no supercritical fluid was escaping the chamber.

For all of the three different types of testing, the final design was used. These tests were selected based on optimization parameters in order to extract the most lipid contents within the fewest time period.

5.3.1 Pressure test

In order to measure the reliability of the procedure, a pressure gauge was purchased and installed in order to accurately measure the pressure. Pressure drops occurred due to supercritical fluid constantly escaping and so heating was performed regularly to maintain the desired pressure.

5.3.2 Temperature test

To measure if the supercritical temperature of CO₂ was reached, a digital probe instant-read thermometer was used to reliably check the temperature of the CO₂ chamber. The thermometer was vertically placed directly on the SFE chamber, and held until temperature stopped fluctuating.

5.3.3 Leaks test

In order to maintain an efficient lipid extraction, pressure had to be constant. If the pressure decreased it would be due to a leak. Therefore, two tests were performed to check for leaks. The first one was manual and involved checking with our fingers for any trace of

leakage on the connections of the CO₂ chamber. If a leak occurred, it would be felt due to the tiny bursts of gas escaping the chamber from the bottom. The second, more accurate, test was performed using a liquid. Because the holding chamber was very cold prior to heating, it formed condensation on the outside. Once heated, this condensation dripped down to the lower connection of the CO₂ chamber. If bubbles were observed at this spot, leaking would be confirmed. These two tests were the only tests that could be performed.

5.4 Experimental setup

After the hydrogel was removed from the Clearing Solution, excess hydrogel was removed and discarded. A picture of the tissue was taken and the tissue was then placed inside the SFE chamber. A copper mesh filter was placed right below it to prevent the tissue from being expelled through the lower valve. Dry ice was then obtained and placed inside the CO₂ chamber, and hammered in to fill in all the empty space. The chamber was then immediately closed once filled, and heated up with a blow torch until supercritical pressure and temperature was reached. The first valve below the lower cap of the CO₂ chamber was opened to allow the supercritical fluid to enter the extraction chamber. The CO₂ chamber was then reheated to bring the pressure back up to the supercritical point. This was performed due to the drop in pressure caused by allowing the fluid to enter the clearing chamber. For our project, we decided to run two different extractions, after 45 minutes and 3 hours. After the designated time, the second valve is opened to allow the supercritical fluid to escape. A container in the form of a metal bucket was used to collect the lipid extract. After all the supercritical fluid has been allowed to escape, the chamber was disassembled and the tissue was collected.

5.5 Transparency Assessment

After doing extraction on tissue using our SFE chamber, we collected the tissue samples and observed them to determine transparency. To do this, prior to doing extraction, we prepared a patterned paper that would help us see any differences in tissue transparency more easily. The first patterned paper we created consisted of twelve rectangular boxes arranged in a 4 x 3 array (rows x columns), where each rectangle was either white or black, yet no two neighboring rectangles had the same color. The length of the rectangles on this patterned paper was about 15mm and their width was about 10mm. The second patterned paper consisted of a pattern of vertical lines with equal spacing between them of about 5mm. This second patterned paper had thinner lines of about 3mm wide and was with the smaller pieces of tissue.

The tissue samples were collected after the extraction was run as described in the Experiment Setup section. The tissue samples were then placed on top of a glass dish. Patterned paper was then placed under the glass that held the tissue. The first type of patterned paper was used for the larger tissue samples, whereas the second type of patterned paper was used for the smaller tissue samples. Several pictures of the tissues with the patterned background were taken. These pictures were then organized and paired by having “Before extraction” and “After extraction” images of the same sample. The degree of transparency was then assessed qualitatively only by comparing the change in color in tissues before and after undergoing supercritical CO₂ extraction.

Chapter 6

Results

This section outlines the results from the experiments with our SFE chamber.

Preliminary results are shown in order to compare and contrast the UV-Vis spectra of the orange extract we obtained in our preliminary studies and the spectra of the known reference limonene. This section also shows the results for the degree of transparency of tissue from two significant extractions.

6.1 Absorbance Test Results

Our team obtained an absorbance plot after collecting the extract from the preliminary studies using oranges. This was done utilizing a UV-Vis spectrophotometer available at the lab. The results of the UV-Vis analysis helped us determine the identity of the extract we obtained from the oranges. The plots shown in the spectrophotometer software were smoothed to reduce noise. One of the filtered plots was then compared with a plot that shows the known absorbance values of limonene. The Figure below shows the two plots.

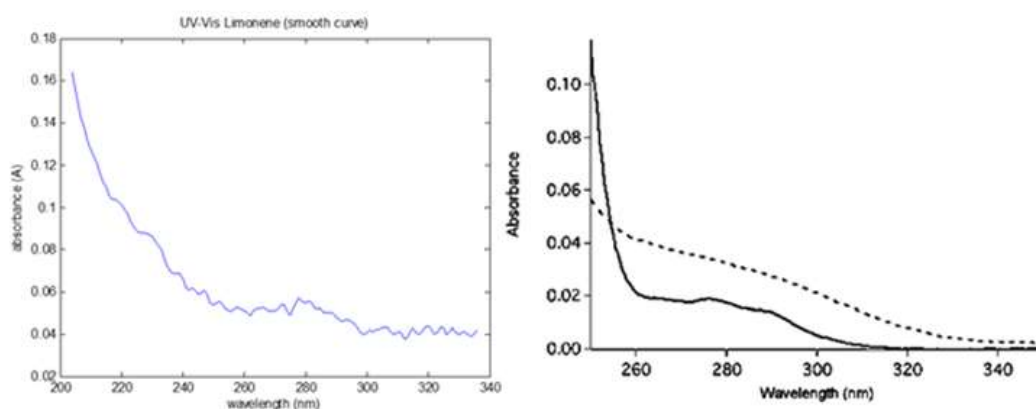


Figure 38: Absorbance plots for the orange oil extract obtained in our experiments (left) and the reference limonene (right). For the plot of the reference limonene, the reference limonene absorbance graph is represented by the solid black line.

Figure 38 shows that the overall shape of the graphs is similar. The absorbance values of our oil extract were higher overall throughout all wavelengths. This is attributed to the fact that the oil we extracted was not purified before sampling in the UV-Vis spectrophotometer.

6.2 Results on SFE Chamber extraction

These images were obtained at different time intervals using the high definition camera of a smart phone. In Figure 39, the upper two are representative of the before and after porcine liver samples were cleared. The thickness was found to be 15 mm and extraction occurred for 45 minutes. In Figure 39, the lower two are representative of the before and after porcine liver samples were cleared. The thickness was found to be 5 mm and extraction occurred for 3 hours.

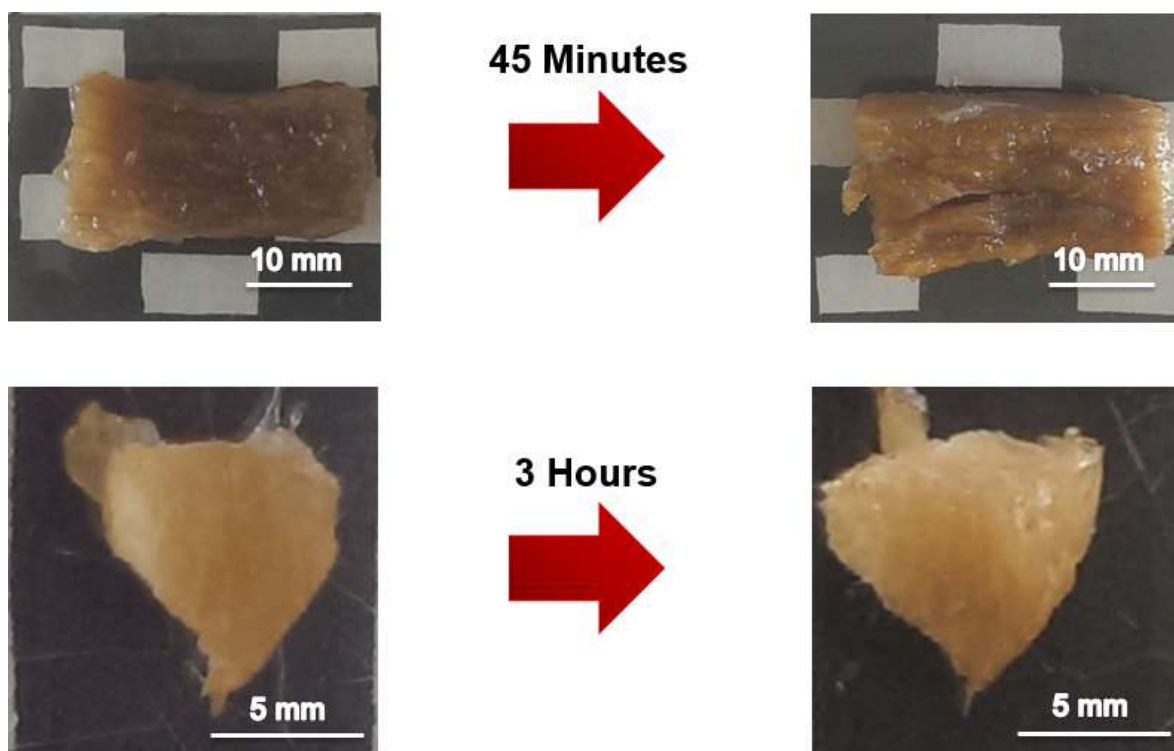


Figure 39: Porcine liver samples before and after extraction.

After supercritical extraction for 45 minutes, the 10 mm sample showed a 5% increase in transparency. This transparency was shown around the edges of the porcine sample and was not significant. However, after supercritical extraction for 3 hours, the 3 mm sampled showed a 40% increase in transparency. Tissue sample was reduced and supercritical fluid exposure time was increased. These factors contributed to such a drastic change in transparency.

Chapter 7

Discussion

The various results obtained in our experiments allowed us to make observations on the effectiveness of supercritical CO₂ in removing lipids from tissue. Our research initially suggested that Supercritical Fluid Extraction (SFE) was an advantageous method in lipid extraction. Since it is a common method utilized in the food industry to extract oils and resins from fruits and plants, it only followed that we did experiments on lipid extraction in animal tissue to assess supercritical fluids' effectiveness in dissolving lipid material. Our preliminary results helped us to determine that the SFE chamber we designed worked well. In fact, it was through the data acquired in these preliminary experiments that we were able to make changes to the design for the subsequent lipid extraction from animal tissue. The results obtained from the extractions done on tissue prove that lipid extraction via SFE is a feasible alternative option to current lipid extraction methods.

The preliminary data gathered from the feasibility studies showed that our SFE chamber initial design was not capable of maintaining pressures as high as CO₂ critical pressure. Though leaking issues with our chamber were quickly addressed by securing connections with military grade tape, issues with the pressure had to be solved differently. The initial component of the CO₂ chamber, the Schedule 80 steel pipe was not rated to have a maximum pressure. And so the team decided to purchase a rated steel pipe having a maximum pressure beyond what was needed for the extraction. Also, the initial acrylic used as the extraction chamber ruptured after the third extraction attempt using vanilla beans. This burst might have happened after continuous extractions by the supercritical CO₂ dissolved the acrylic chamber. We believe that the imperfection that the acrylic chamber had after being machined at the lathe caused micro-ruptures in the acrylic chamber that later facilitated CO₂ to diffuse through the chamber. Thus, the acrylic chamber was changed in favor of a stronger aluminum chamber for the final design.

The preliminary data for the oil extract we obtained from the oranges showed us that its composition was very similar to the natural orange oil, limonene. These data revealed that the absorbance values of our extract resembled the absorbance values of limonene in a significant way. Though the absorbance plot obtained from the UV-Vis software was not identical to the reference absorbance plot, the shape of the plot provided enough evidence to conclude that our extract was composed of lipid material.

The design was successful in that our goal of improving the transparency of the porcine tissue sample was accomplished. The original objective was a 10% improvement but we believe the chamber was more efficient and that an improvement of 40% was actually reached. However, the tissue sample was not as transparent as other methods such as CLARITY. The only pictures available for comparison in CLARITY, Scale, and SeeDB generally comprised of a “before” and “after”. Because none of these methods had images after 45 minutes, or 3 hours, there was no legitimate way to directly assess the effectiveness of our chamber. However, we believe our chamber does not take as long as two weeks to clear tissue due to the 40% improvement which was performed in under a day, a fraction of the time compared to 14 days. The complexity of our design was between CLARITY’s intricate procedure and Scale/SeeDB’s simple method. CLARITY created a customized chamber that uses electrophoresis to remove lipid, and voltage was administered throughout the tissue within a solution. This solution had to be replaced over time in order to remove the lipid extracts from the clearing solution due to the reduction in clearance effect. Scale and SeeDB were relatively simple due to the fact that the tissue was only immersed in a solution. Scale was placed in a urea-based solution and SeeDB was placed in a fructose solution. Both of these were incubated in a solution and agitated, and the solution did not have to be replaced. Our design was in between these approaches difficulty-wise due to the fact that we had to place dry ice into a chamber and manually heat it, but we did not have to run it for too long. Because

it was relatively fast to obtain results, it was a simple procedure due to lack of maintenance required.

When it came to creating a design, each of the three current methods of removing lipids was scrutinized. The biggest drawbacks for each were examined and it was found that for CLARITY, 8% of total protein was lost. This is a huge downside because this would affect fluorescent staining. All of the proteins are not conserved, and so when imaging occurs, the visual representation would not be accurate. CLARITY has the least total protein loss, with Scale having a 41% loss. Scale also has issues with maintaining structural integrity. Swelling occurs every time, and to decrease swelling, incubation time must be increased to 6 months to prevent any swelling at all. After fluorescent staining, this creates flawed imaging as well. SeeDB has the drawback of having browning occur, which is due to the fructose. All of these drawbacks led to us creating a different method of inducing transparency. Supercritical CO₂ became the desired method for our team not only because of the lipid extraction strength and efficiency, but also because of the complexity of current systems becoming an issue. We decided to use dry ice instead of complex pumps and tanks due to our budget and time. Dry ice is just condensed, solidified carbon dioxide, and we only needed to heat it to create our desired supercritical fluid. Dry ice was also relatively cheap in bulk, and could be broken into tiny pieces to fit inside our chamber.

Chapter 8

Conclusions and Future Recommendations

The results obtained in our experiments show that our SFE chamber has potential to be used as a model for lipid extraction from tissues. In the feasibility studies, our device was capable of removing oils from orange peels. These oils also proved to be similar to the oil known to be extracted from oranges in industries. In the experiments done with porcine tissue, our device successfully managed to extract lipids while keeping the tissue almost intact after extraction. Nonetheless, our team experienced challenges when running the experiments. Examples include the acrylic chamber bursting during preliminary testing, the leaking caused by improper tightening, and the constant heating of the CO₂ chamber. Even though some issues arose with regards to the assembly itself, the device showed great efficacy by making tissue transparent at almost 40% according to our advisor. Regardless of the success of the project, the team identified a few ways in which the concept tested in our project can be up-scaled possibly used in clinical applications in the future.

8.1 Add Heating system

To reach the critical temperature of CO₂, our team heated the SFE chamber with a propane blow torch. Heating the CO₂ chamber this way took quite some time. Due to the concentrated heat being applied to one point of the SFE chamber, temperatures inside the chamber must have varied. It is suggested that a self-controlling heating tape be wrapped around the chamber to equally heat the CO₂ chamber. This heating tape would maintain the heat constant throughout the chamber. This would also allow the chamber to be left alone for long periods of time which would allow for longer extractions and better results. This heating tape would need to be strong enough to heat up a Schedule 160 steel pipe. This would work in conjunction with a system for replenishing the dry ice.

8.2 Incorporate self-refilling dry ice

A huge drawback of our design was the relatively short amount of time that the SFE chamber was active. A person also had to be constantly reheating the chamber every five to ten minutes due to the loss of pressure caused by leakage. The leakage was caused by the fluid bypassing the wrapping tape used to cover the pipe threads. If leaking cannot be prevented, a system is needed that would enable more dry ice to be placed inside the chamber. This would compensate for the escaping fluid because more supercritical fluid would be created. The mechanism needed would be spring-loaded and it would need to sense when the pressure cannot rise anymore. If the pressure could not go up any higher, then it would be because there would be no carbon dioxide left in the chamber. The spring-loaded system would then add in more dry ice.

8.3 Improve Closing mechanism

The current design is based off a Schedule 160 pipe with external threads caps. The threaded ends of the pipe were wrapped in tape in order to help create a tighter fit before screwing the caps to the pipe. Once caps and pipe were assembled together, we observed that no matter how much tape was used, leaking always occurred. Supercritical CO₂ has a high diffusivity and low density, so it should be able to tear through the tape quite easily. However, we had to prevent as much leaking as possible. A better system would use a vacuum based cap that would only get tighter as the higher the pressure rises. This cap would tighten the higher the pressure is. It would allow the possibility of air to be vacuumed out of the chamber. This would enable more CO₂ particles to fit into the chamber and maximize extraction efficiency.

8.4 Expand SFE chamber

Tissue sample size was decreased in our design, in order to improve extraction results. Another option however is to increase the size of the extraction chamber, which would also improve clearance efficiency. Larger samples could be placed inside the chamber, and possibly whole-tissue samples. Enabling lipid extraction in large scale SFE chamber could then improve the overall efficiency of the design in making tissue transparent.

8.5 Implementing Fluorescent Staining

Ideally our design would need to be able to extract lipids out of tissue that would allow for whole tissue staining using fluorescent probes. By making tissue transparent we would be able to allow light to go through the entire sample. This would then allow us to incorporate a fluorescent tagging technique to visualize the proteins within the tissue sample. If this is the case, then different molecules could be tagged with different colors thus allowing for proper identification of the molecular composition of the tissue.

References

1. "Cancer Fact Sheet No 297." WHO. World Health Organization, Jan. 2013. Web. 27 Sept. 2013. <<http://www.who.int/mediacentre/factsheets/fs297/en/>>.
2. Sircus, Mark. "Cost of Cancer Treatments - Natural Allopathic Vs. Allopathic." Dr. Sircus. International Medical Veritas Association, 2 Jan. 2013. <<http://drsircus.com/medicine/cancer/cost-cancer-treatments-natural-allopathic-allopathic>>.
3. "Heredity and Cancer." Heredity and Cancer. American Cancer Society, 27 Dec. 2011. Web. 27 Sept. 2013. <<http://www.cancer.org/cancer/cancercauses/geneticsandcancer/heredity-and-cancer>>.
4. "What Is Cancer? What Causes Cancer?" Medical News Today. Medi Lexicon International, n.d. Web. 27 Sept. 2013. <<http://www.medicalnewstoday.com/info/cancer-oncology/>>.
5. "Treatment Types." Types of Cancer Treatment. American Cancer Society, n.d. Web. 11 Sept. 2013.
6. "Program Overview - TCGA." Cancer Genome NIH. National Human Genome Research Institute, n.d. Web. 27 Sept. 2013. <<http://cancergenome.nih.gov/abouttcga/overview>>.
7. "Western Blotting (immunoblot): Gel Electrophoresis for Proteins." Antibodies-Online. N.p., n.d. Web. 27 Sept. 2013. <[http://www.antibodies-online.com/resources/17/1224/Western blotting immunoblot Gel electrophoresis for proteins](http://www.antibodies-online.com/resources/17/1224/Western%20blotting%20immunoblot%20Gel%20electrophoresis%20for%20proteins)>.
8. Chung, Kwanghun, and Karl Deisseroth. "CLARITY for Mapping the Nervous System." *Nature* 10.6 (2013): 508-14.
9. Hama, Hiroshi, Hiroshi Kurokawa, and Hiroyuki Kawano. "Scale: A Chemical Approach for Fluorescence Imaging and Reconstruction of Transparent Mouse Brain." *Nature Neuroscience* 14.11 (2011): 1481-488.
10. "Cancer Facts and Statistics." American Cancer Society. N.p., n.d. Web. 15 Oct. 2013. <<http://www.cancer.org/research/cancerfactsstatistics/>>.
11. Anand, Preetha. "Cancer Is a Preventable Disease That Requires Major Lifestyle Changes." National Center for Biotechnology Information. U.S. National Library of Medicine, n.d. Web. 15 Oct. 2013. <<http://www.ncbi.nlm.nih.gov/pubmed/18626751>>.
12. Strahan, T. "Human Molecular Genetics." National Center for Biotechnology Information. U.S. National Library of Medicine, n.d. Web. 15 Oct. 2013. <<http://www.ncbi.nlm.nih.gov/pubmed/21089233>>.
13. Roukos, D. H. "Genome-wide Association Studies: How Predictable Is a Person's Cancer Risk?" National Center for Biotechnology Information. U.S. National Library of

- Medicine, n.d. Web. 15 Oct. 2013.
<<http://www.ncbi.nlm.nih.gov/pubmed/19374592>>.
14. Svobodová AR, Galandáková A, Sianská J, et al. (January 2012). "DNA damage after acute exposure of mice skin to physiological doses of UVB and UVA light".
 15. David S. Goodsell (2001). "The Molecular Perspective: Ultraviolet Light and Pyrimidine Dimers". *The Oncologist* 6 (3): 298–299
 16. "DNA_UV_mutation." Wikipedia. Wikimedia Foundation, n.d. Web. 15 Oct. 2013.
<http://en.wikipedia.org/wiki/File%3ADNA_UV_mutation.svg>.
 17. "Checkpoint Inhibitor Sensitizes Human Tumor Cells." *In the Journals*. National Cancer Institute, n.d. Web. 15 Oct. 2013.
<<http://home.ccr.cancer.gov/inthejournals/mitchell.asp>>.
 18. Markowitz SD, Bertagnolli MM (December 2009). "Molecular basis of colorectal cancer". *N. Engl. J. Med.* 361 (25): 2449–60
 19. "Signs and Symptoms of Cancer." *Cancer*. American Cancer Society, n.d. Web. 15 Oct. 2013. <<http://www.cancer.org/cancer/cancerbasics/signs-and-symptoms-of-cancer>>.
 20. "Possible Symptoms of Cancer." : Cancer Research UK : CancerHelp UK. N.p., n.d. Web. 15 Oct. 2013. <<http://www.cancerresearchuk.org/cancer-help/about-cancer/causes-symptoms/possible-symptoms-of-cancer>>.\
 21. "The Cost of Cancer." *National Cancer Institute*. N.p., n.d. Web. 15 Oct. 2013.
<<http://www.cancer.gov/aboutnci/servingpeople/cancer-statistics/costofcancer>>.
 22. "Avastin (Bevacizumab) Price." Avastin (Bevacizumab) Price. News Medical, n.d. Web. 15 Oct. 2013. <<http://www.news-medical.net/health/Avastin-%28Bevacizumab%29-Price.aspx>>.
 23. "Radiation Therapy Cost." CostHelper Health. N.p., n.d. Web. 15 Oct. 2013.
<<http://health.costhelper.com/radiation-therapy.html>>.
 24. "Treatment Types." Cancer. American Cancer Society, n.d. Web. 15 Oct. 2013.
<<http://www.cancer.org/treatment/treatmentsandsideeffects/treatmenttypes/index>>.
 25. "Questions about Chemotherapy." Cancer. American Cancer Society, n.d. Web. 15 Oct. 2013.
<<http://www.cancer.org/treatment/treatmentsandsideeffects/treatmenttypes/chemotherapy/whatitishowithelps/chemo-what-it-is-questions-about-chemo>>.
 26. "Different Types of Chemotherapy Drugs." Cancer. American Cancer Society, n.d. Web. 15 Oct. 2013.
<<http://www.cancer.org/treatment/treatmentsandsideeffects/treatmenttypes/chemotherapy/chemotherapyprinciplesanin>>.

depthdiscussionofthetechniquesanditsroleintreatment/chemotherapy-principles-types-of-chemo-drugs>.

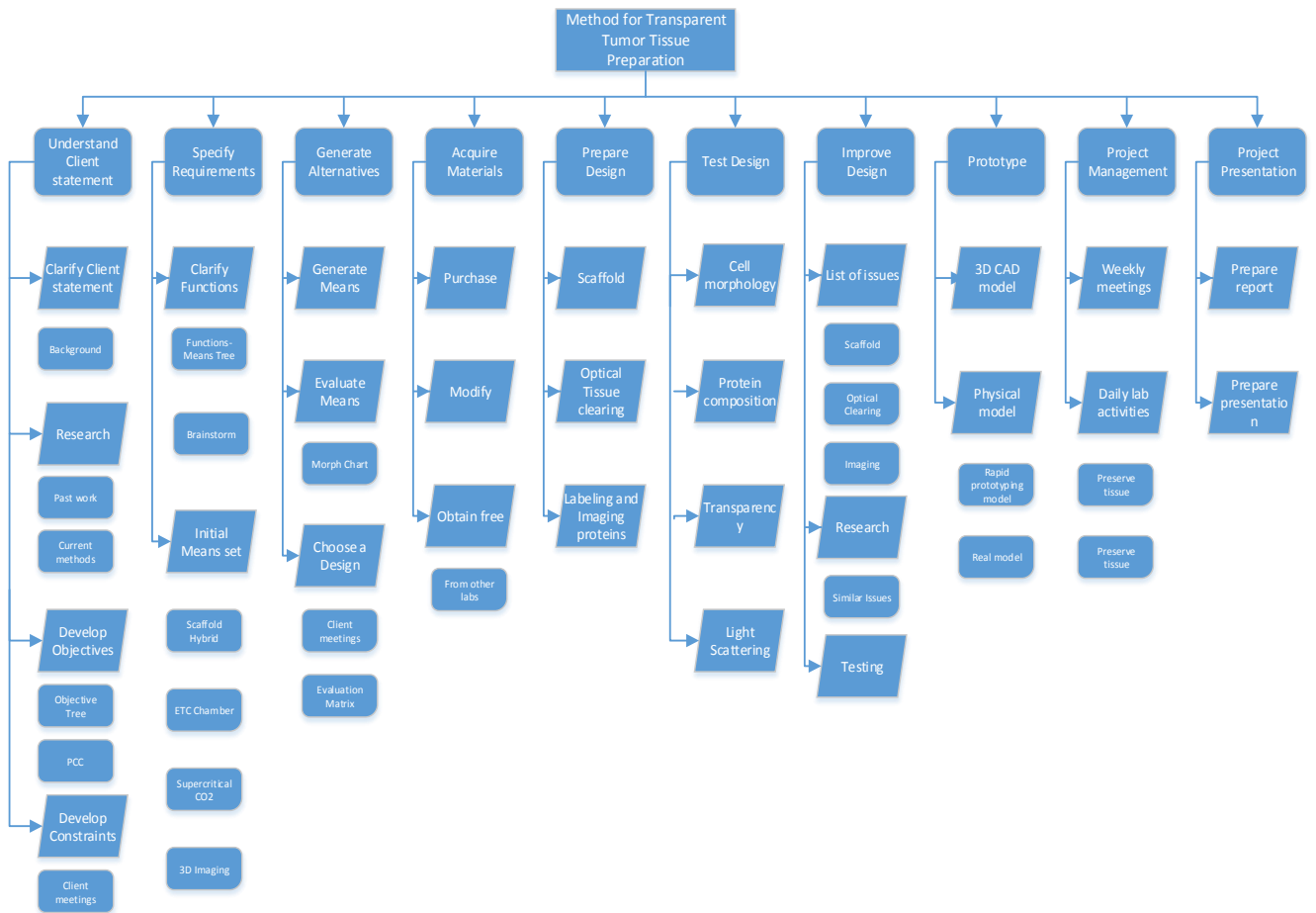
27. "Figure 2. Chemotherapy Targets." Nature.com. Nature Publishing Group, n.d. Web. 15 Oct. 2013.
<http://www.nature.com/nature/journal/v438/n7070/fig_tab/nature04483_F2.html>.
28. "Questions about Radiation Therapy." Cancer. American Cancer Society, n.d. Web. 15 Oct. 2013.
<<http://www.cancer.org/treatment/treatmentsandsideeffects/treatmenttypes/radiation/radiationtherapy-whatitishowithelps/radiation-therapy-what-it-is-questions-about-rad-therapy>>.
29. "Types of Radiation Used to Treat Cancer." Cancer. American Cancer Society, n.d. Web. 15 Oct. 2013.
<<http://www.cancer.org/treatment/treatmentsandsideeffects/treatmenttypes/radiation/radiationtherapyprinciples/radiation-therapy-principles-types-of-radiation>>.
30. "External Beam Radiation Therapy." Cancer.gov. National Cancer Institute, n.d. Web. 15 Oct. 2013. <<http://www.cancer.gov/cancertopics/coping/radiation-therapy-and-you/page3>>.
31. "How Is Surgery Used for Cancer?" *Cancer*. American Cancer Society, n.d. Web. 15 Oct. 2013.
<<http://www.cancer.org/treatment/treatmentsandsideeffects/treatmenttypes/surgery/surgery-how-is-surgery-used-for-cancer>>.
32. "Types of Immunotherapy." Cancer. American Cancer Society, n.d. Web. 15 Oct. 2013.
<<http://www.cancer.org/treatment/treatmentsandsideeffects/treatmenttypes/immunotherapy/immunotherapy-types>>.
33. Cikes, M., and Klein, G. Quantitative studies of antigen expression in cultured murine lymphoma cells. I. Cell-surface antigens in asynchronous cultures. *J. Natl. Cancer Inst.*, 49: 1599-1606, 1972.
34. Griffen, J. E., Aliman, D. R., Durrani, J. L., and Wilson, J. D. Variation in steroid 5 α reductase activity in cloned human skin fibroblasts. *J. Biol. Chem.*, 256: 3662-3666, 1981.
35. Nowell, P. C. The clonal evolution of tumor cell populations. *Science (Wash. DC)*, 194: 23-28, 1976.
36. Isaacs, J. T., Wake, N., Coffey, D. S., and Sandberg, A. A. Genetic instability coupled to clonal selection as a mechanism for tumor progression in the Dunning R-3327 rat prostatic adenocarcinoma system. *Cancer Res.*, 42:2353-2361, 1982.
37. Frost, P., and Kerbel, R. S. On the possible epigenetic mechanism(s) of tumor cell heterogeneity. *Cancer Metastasis Rev.*, 2: 375-378, 1984.

38. Heppner, Gloria H. "Tumor Heterogeneity." *Cancer Research* 44 (1984): 2259-265. American Association for Cancer Research.)
39. Cifone, M., and Fidler, I. J. Increasing metastatic potential is associated with increasing genetic instability of clones isolated from murine neoplasms. *Proc. Nati. Acad. Sci. USA*, 78. 6249-6252, 1981.
40. Omar, R. A., and tanks, K. W. Origin of phenotypic variation in clones of simian virus 40-transformed mouse embryo eels. *Cancer Res.*, 43: 1835-1841, 1983.
41. Watts, Raymond G., and Kerry Parsons. "Chemotherapy Medication Errors in a Pediatric Cancer Treatment Center." *Pediatr Blood Cancer* 60 (2013): 1320-324. Wiley Periodicals, Inc.
42. Sircus, Mark. "Cost of Cancer Treatments - Natural Allopathic Vs. Allopathic." Dr. Sircus. International Medical Veritas Association, 2 Jan. 2013. <<http://drsircus.com/medicine/cancer/cost-cancer-treatments-natural-allopathic-allopathic>>.)
43. Godman, Brian, Alexander Finlayson, Parneet Cheema. "Personalizing health care: feasibility and future implications." *BMC Medicine* (2013) 11:179.
44. "StudyDroid." StudyDroid. N.p., n.d. Web. 15 Oct. 2013. <<http://www.studydroid.com/printerFriendlyViewPack.php?packId=19735>>.
45. Alberts, Bruce. "The Lipid Bilayer." NCBI. U.S. National Library of Medicine, 18 Feb. 2000. Web. 15 Oct. 2013. <<http://www.ncbi.nlm.nih.gov/books/NBK26871/>>.
46. "What Are Tumor Markers?" Cancer. American Cancer Society, n.d. Web. 15 Oct. 2013. <<http://www.cancer.org/treatment/understandingyourdiagnosis/examsandtestdescriptions/tumormarkers/tumor-markers-what-are-t-m>>.
47. "Level of Tumor Protein Indicates Chances Cancer Will Spread, February 1, 2011 News Release - National Institutes of Health (NIH)." NIH. U.S. National Library of Medicine, n.d. Web. 15 Oct. 2013. <<http://www.nih.gov/news/health/feb2011/nichd-01.htm>>.
48. "ELISA (Enzyme-Linked ImmunoSorbant Assay)." ELISA Method. Bio Davidson, n.d. Web. 15 Oct. 2013. <<http://www.bio.davidson.edu/genomics/method/ELISA.html>>.
49. Towbin H, Staehelin T, Gordon J. (1979). "Electrophoretic transfer of proteins from polyacrylamide gels to nitrocellulose sheets: procedure and some applications". *Proceedings of the National Academy of Sciences USA* 76 (9): 4350-54.).
50. "Methods for Imaging Thick Specimens: Confocal Microscopy, Deconvolution, and Structured Illumination." CSH Protocols. Cold Spring Harbor Protocols, n.d. Web. 15 Oct. 2013. <<http://cshprotocols.cshlp.org/content/2011/12/pdb.top066936.full>>.

51. Bryner, Jeanna. "Scientists Create See-Through Fish, Watch Cancer Grow." LiveScience.com. N.p., 06 Feb. 2008. Web. 15 Oct. 2013. <<http://www.livescience.com/2267-scientists-create-fish-watch-cancer-grow.html>>.
52. Szot, Christopher, Cara Buchanan, and Joseph Freeman. "3D in Vitro Bioengineered Tumors Based on Collagen I Hydrogels." *Biomaterials* 32 (2011): 7905-912.
53. "Optical Clearing Agent SCALEVIEW A2." Olympus UIS2 Series for Biological Microscopes. Olympus, n.d. Web. 15 Oct. 2013. <<http://microscope.olympus-global.com/uis2/en/scaleview/>>.
54. "Refractive Index." Wikipedia. Wikimedia Foundation, 10 Sept. 2013. Web. 15 Oct. 2013. <http://en.wikipedia.org/wiki/Refractive_index>.
55. Ke, Meng-Tse. "SeeDB: a simple and morphology-preserving optical agent for neuronal circuit reconstruction". *Nature Neuroscience*. 16 (8) 2013, pp. 1154-63
56. "Supercritical Fluid." Wikipedia. Wikimedia Foundation, 28 Sept. 2013. Web. 15 Oct. 2013. <http://en.wikipedia.org/wiki/Supercritical_fluid>.
57. "Supercritical Fluids - 2. The Use of Supercritical Fluid Extraction Technology in Food Processing." Supercritical Fluids -Elecsus. N.p., n.d. Web. 15 Oct. 2013. <<http://eng.ege.edu.tr/~otles/SupercriticalFluidsScienceAndTechnology/bolumb/Wc34c920327cd9.htm>>.
58. Sahena, F., and I. S. Zaidul. "Application of Supercritical CO2 in Lipid Extraction – A Review." *Journal of Food Engineering* 95. 2 (2009): 240-53.
59. Cutler, S. "Natural Extracts Using Supercritical Carbon Dioxide By Mamata Mukhopadhyay". *Journal of Natural Products*, 64. 5 (2001), p. 691.
60. Krasnow, Ben. "Supercritical CO2 Extraction of Cinnamon, Coffee, and Vanilla with Dry Ice." Applied Science (2013). Web. <<https://www.youtube.com/watch?v=UxAjlmaUNzs>>.
61. Chun, K., Wallace, J., Kim S. et al. "CLARITY Protocol". Stanford University (2013). Pp. 1-2

Appendix

Work Breakdown Structure



Cost Analysis (For ETC)

Item	Estimated Cost	Description
Scaffold fabrication-Scaffold material	\$30-\$100	Cost based on acrylamide monomers pricing.
Scaffold fabrication-Crosslinking agent	\$30-\$50	Cost based on formaldehyde pricing.
Scaffold fabrication- Tumor tissue	\$400-\$500	Cost based on mouse and human tissue lines.
Optical clearing method-Chamber materials	\$20-\$40	Cost based on the pricing of materials needed to build the ETC (Nalgene, platinum wires, epoxy, aluminum)
Optical clearing method-Supercritical CO ₂ pump	\$3000	Cost based on the ISCO SUPREX SCF Extraction Pump
Optical clearing method-reagent/solvent	\$65-\$120	Cost based on the SDS reagent pricing
Imaging-antibodies	\$300	Cost based on antibodies from Sigma Aldrich
Imaging- microscope	\$0	Microscope equipment is already in the laboratory
Prototyping-Rapid prototyping model	\$30	Cost based on the estimation of the cost associated in building a small prototype
Prototyping- Actual prototype	\$70	Cost based on the pricing of materials needed to build the chamber
Expected cost of design	\$85	Based on modification on the actual prototype

Hydrogel Preparation Protocol

Hydrogel Materials

- 40 mL of Acrylamide (40%), with final concentration of 4%
- 10 mL of Bisacrylamide (2%), with final concentration of 0.05%
- 40 mL of 10X PBS, with final concentration of 1X
- 100 mL of PFA (16%), with final concentration of 4%
- 210 mL of dH₂O
- 1 g of VA-044 Initiator, with final concentration of .25%

Creates 400 mL of hydrogel monomer solution.

Everything must be kept on ice, store at -20 C until ready to be used.

Place the tissue in cold hydrogel solution, on ice until it can be moved to a 4°C refrigerator.

Incubate at 4°C for 2-3 days to allow for further diffusion of the hydrogel solution into the tissue.

Hydrogel Embedding

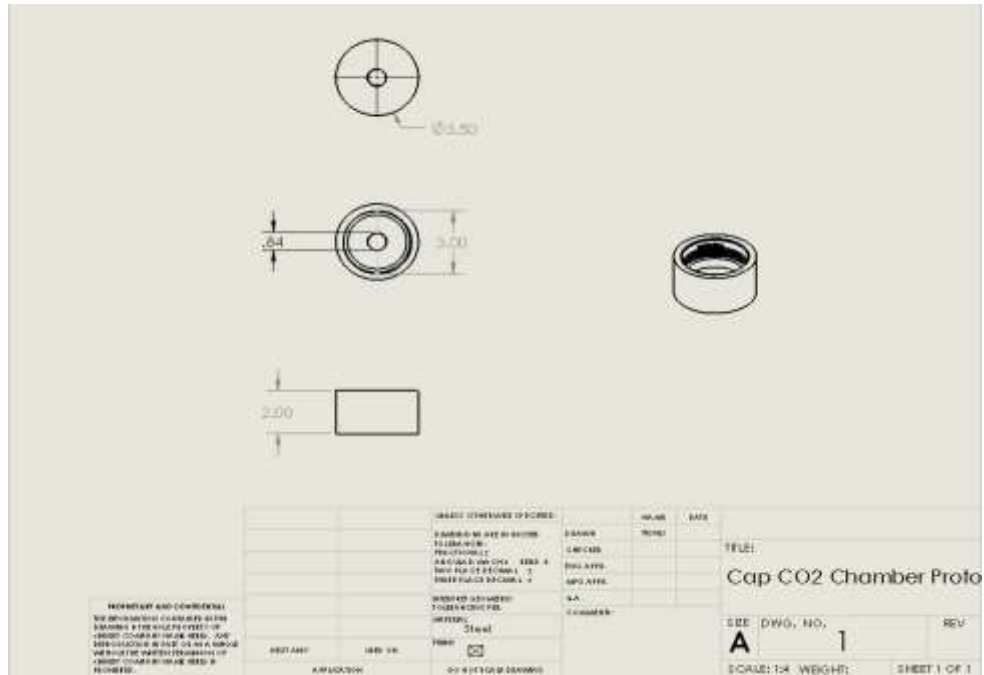
1. De-gas solution (in container) in a fume hood, to replace oxygen with nitrogen (oxygen prevents hydrogel formation)
 - Place container in fume hood, and open container to allow gas exchange
 - Turn on nitrogen tank, and adjust control valve so the inlet to the fume hood fills with nitrogen
 - Switch the fume hood valve from nitrogen gas flow to the vacuum
 - Turn on the vacuum pump, and allow it to run for 10 minutes
 - Turn off vacuum and slowly turn the valve to fill the chamber with nitrogen
 - Carefully open the chamber just enough to reach the tubes while purging with nitrogen gas. Taking great care to minimize exposure to air, and quickly and tightly close the sample container.
2. Place container in 37°C water bath, or incubate it. This must be done for 3 hours until solution has polymerized.
3. In a fume hood, extract the embedded sample from the gel, using gloves.
4. Wash samples with 50 mL of “Clearing Solution” for 24 hours at room temperature to get rid of extra PFAS, initiator, and monomer. This is repeated two more times.

Clearing Solution Materials

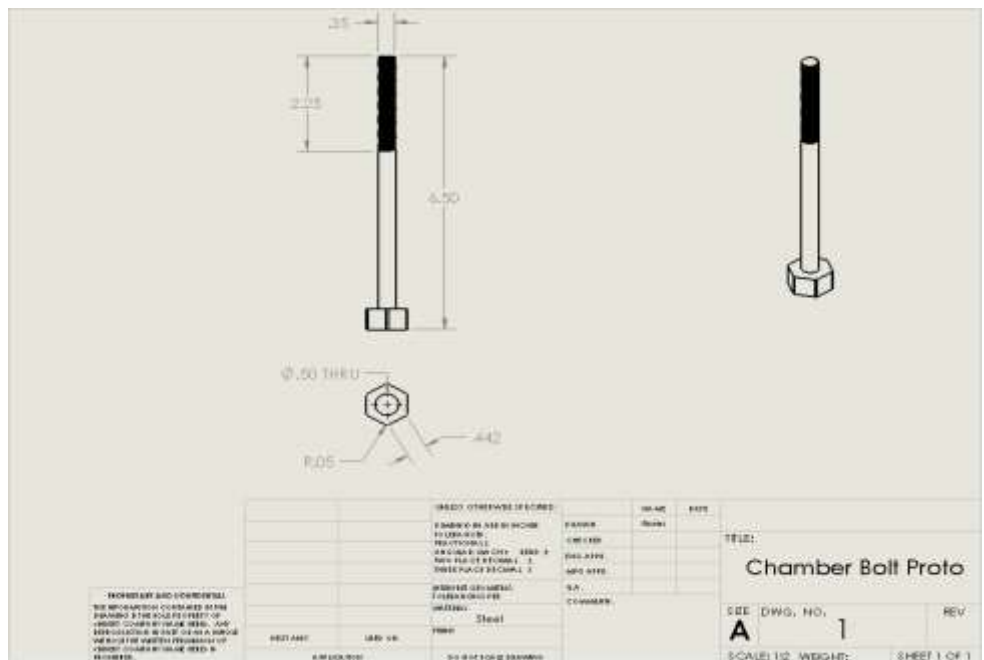
- 123.66 g of Boric Acid, with final concentration of 200 mM
- 400 g of Sodium Dodecyl Sulfate (SDS) with final concentration of 4%
- dH₂O is added until 10 L mark
- NaOH is added until pH is at 8.5

This creates 10 L, which is 10,000 mL. We only need 150 mL (3 times of washing sample).

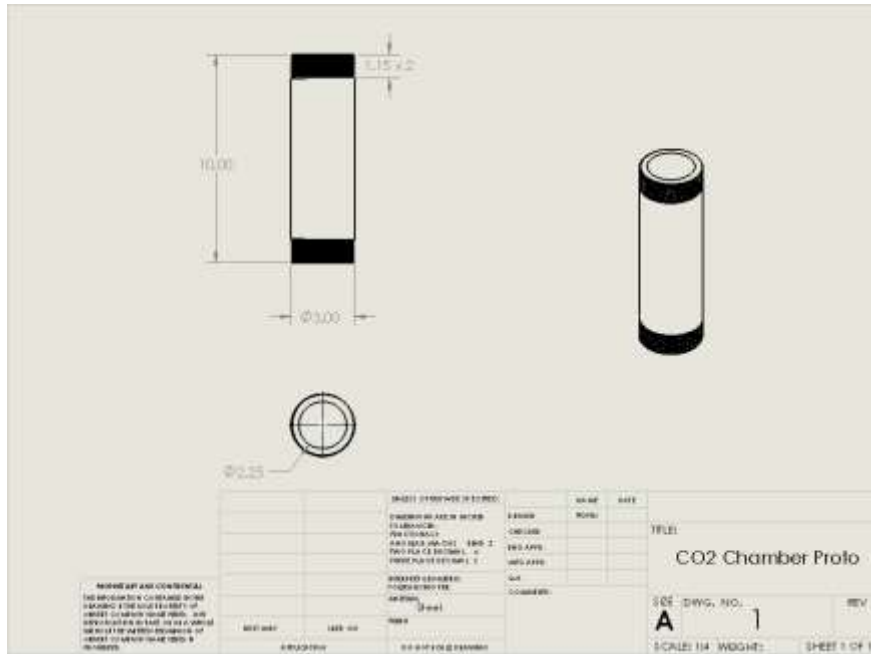
CAD Drawing of Cap of the CO₂ chamber



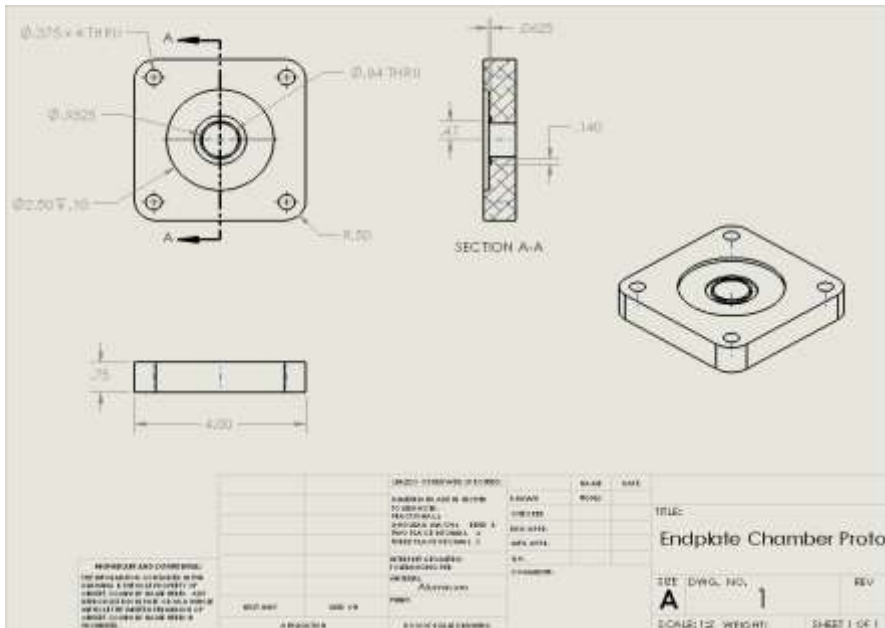
CAD Drawing of the bolts used to hold endplates of the extraction chamber



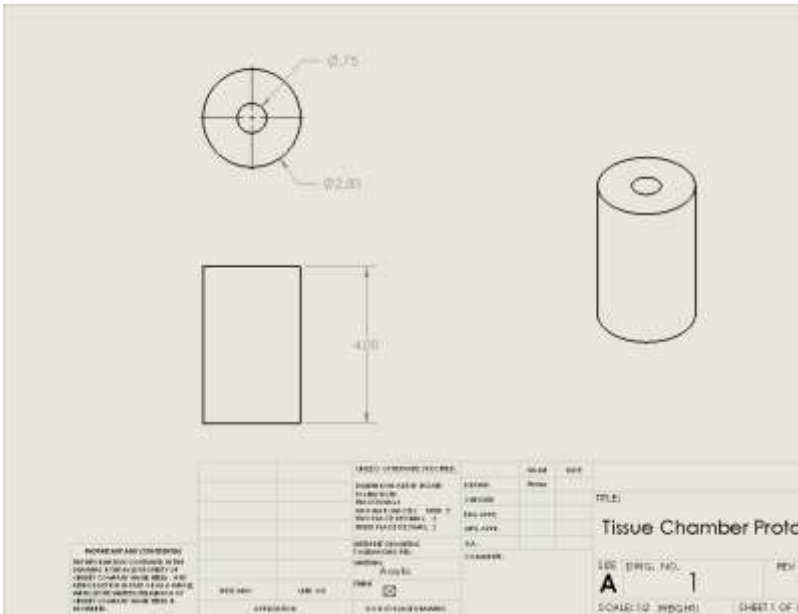
CAD Drawing of the CO₂ chamber



CAD Drawing of the endplate of the extraction chamber



CAD Drawing of the extraction chamber



Final CAD model of the SFE chamber assembly

